Hotspots for warm and dry summers in Romania

1   Viorica Nagavciuc[1,2], Patrick Scholz[1] and Monica Ionita[1,3*]

2   [1]Alfred Wegener Institute Helmholtz Center for Polar and Marine Research, Paleoclimate Dynamics Group, Bremerhaven,
3   Germany

4   [2]Faculty of Forestry, Ștefan cel Mare University, Suceava, Romania

5   [3]Emil Racovita Institute of Speleology, Romanian Academy, Cluj-Napoca, Romania
6
7   *** Correspondence:**
8
9   Monica.Ionita@awi.de

11   **Keywords: heatwaves, drought, compound events, atmospheric circulation, climate change.**

12   **Abstract**

13   The combined effect of hot and dry extremes can have disastrous consequences for the society, economy, and the environment.
14   While a significant number of studies have been conducted regarding the variability of the individual hot or dry extremes in
15   Romania, the evaluation of the combined effect of these extremes (e.g. compound effect) is still lacking for this region. Thus,
16   in this study, we have assessed the spatio-temporal variability and trends of hot and dry summers in Romania, between 1950
17   and 2020 and we have analyzed the relationship between the frequency of hot summers and the prevailing large-scale
18   atmospheric circulation. The length, spatial extent, and frequency of Heat Waves (HWs) in Romania present decadal
19   variations, the rate of increase being accelerated after the 1990's. The smallest number of HWs was observed between 1970
20   and 1985, while the highest number of HWs has been recorded over the last two decades (i.e. 2001 – 2020). The hottest years,
21   in terms of heatwave duration and frequency, were 2007, 2012, 2015, and 2019. One of the key drivers of hot summers, over
22   our analyzed region, is the prevailing large-scale circulation, featuring an anticyclonic circulation over the central and eastern
23   parts of Europe and enhanced atmospheric blocking activity associated with positive temperature anomalies underneath. The
24   results from this study can help improve our understanding of the spatio-temporal variability of hot and dry summers over
25   Romania, as well as their driving mechanisms which might lead to a better predictability of these extreme events in the region.

1 Introduction

According to the recently published AR6 report (IPCC, 2021): "It is virtually certain that there has been increases in the intensity and duration of heatwaves and the number of heatwave days at the global scale". This tendency has been clearly observed, especially over the last two decades, when a significant increase in the frequency of hot summers has been observed (Feng et al., 2020; Raymond et al., 2020; Seneviratne et al., 2012; Zscheischler et al., 2018). Moreover, one of the main conclusions of the recently published IPCC AR6 report (IPCC, 2021) was that "future heatwaves will last longer and have higher temperatures". In this report (and the references therein) it has been shown that on a global scale there is clear evidence of an increase in the number of warm nights and days and a decrease in the number of cold nights and days (IPCC, 2021). Overall, the frequency of warm days (TX90p) has increased globally with small exceptions in the southern part of South America (IPCC, 2021; Rusticucci et al., 2017). Over Europe, an increase in the magnitude and frequency of high maximum temperatures has been observed over central (Lorenz et al., 2019; Tomczyk and Bednorz, 2016; Twardosz and Kossowska-Cezak, 2013) and the southern-eastern part of Europe (Christidis et al., 2015; Croitoru et al., 2016a; Croitoru and Piticar, 2013; Fioravanti et al., 2016; Malinovic-Milicevic et al., 2016).

Over different regions of the world, hot summers are usually accompanied by extremely dry conditions, leading to the development of the so-called "compound events" (Feng et al., 2020; Geirinhas et al., 2021; Leonard et al., 2014; Ridder et al., 2020; Russo et al., 2019). These compound events have the tendency to occur at the same time or in sequence, leading to devastating consequences for the society, economy, and environment (Raymond et al., 2020; Zscheischler and Seneviratne, 2017). Heatwaves and droughts fall into the category of climate related hazards which affect more and more frequently socio-economic activity, often having serious repercussions on humans and the environment (IPCC, 2021). Thus, in the context of the ongoing climate change, the analysis of heatwaves and droughts, in terms of changes in their frequency and magnitude as well as the analysis of the large-scale circulation patterns which favor their occurrence, is of increasing interest (Balting et al., 2021; Feng et al., 2020; Geirinhas et al., 2021; Ionita et al., 2021a; Kong et al., 2020; Russo et al., 2019).

Several studies have suggested that due to global warming the large-scale atmospheric circulation has been altered both regionally and globally (Horton et al., 2015; Vaideanu et al., 2020). Any perturbance in the large-scale atmospheric circulation will also lead to changes in the hydroclimate, due to the fact that the atmospheric circulation plays a crucial role in the global and regional hydroclimatic variability (Ionita et al., 2020; Kingston et al., 2006, 2015; Schubert et al., 2016). Changes in temperature and precipitation have been found to be a direct response to changes in the large-scale atmospheric circulation patterns (e.g. an increase in the frequency of blocking conditions or an intensification of the westerlies) (Horton et al., 2015; Rimbu et al., 2014; Swain et al., 2016). For example, one key driver of the European hydroclimate variability is the prevalence of long-lasting high-pressure systems (also known as atmospheric blocking) (Bakke et al., 2020a; Barriopedro et al., 2011; Ionita et al., 2021b; Kautz et al., 2021; Rimbu et al., 2014; Schubert et al., 2014). These long-lasting high-pressure systems have a significant impact on different types of extreme events such as heatwaves (Barriopedro et al., 2011; Della-Marta et al., 2007; Laaha et al., 2017), cold spells (Jeong et al., 2021; Rimbu et al., 2014), droughts (Ionita et al., 2012; Kingston et al., 2015; Schubert et al., 2016) and floods (Grams et al., 2014; Najibi et al., 2019). Thus, it is essential to study the relationship between the changes in the magnitude and frequency of extreme events and their large-scale drivers, in order to have a better overview of the physical mechanisms leading to the occurrence of these extreme events.

In terms of exposure and vulnerability to such climate-related risks (e.g. heatwaves and droughts), Romania is particularly prone, both due to its geographical position, as well as the topographic features, which give it a very special status in relation to the manifestations of the weather (Croitoru and Piticar, 2013; Micu et al., 2021; Sfîcă et al., 2017). The existence of the Black Sea and, especially, the concentric distribution (i.e. "in the amphitheater") of the Carpathian Mountains (Figure 1), induce a series of peculiarities in the prevailing climatic conditions that are also reflected in the thermal regime mediated at the scale of different regions of the country. Moreover, the evolution of the weather in Romania depends strongly on the degree of exposure to alternating, often rapid, types of air masses passing the country (e.g. continental, tropical, maritime, or polar) (Bădăluță et al., 2019; Busuioc et al., 2010, 2015; Tomozeiu et al., 2005).

At country scale, different studies have analyzed the potential changes in the frequency of HWs, either by using observational records (e.g. station data) or gridded datasets (Croitoru et al., 2016b; Croitoru and Piticar, 2013; Hustiu, 2016; Micu et al., 2021; Sfîcă et al., 2017). In their paper, Sfîcă et al. (2017) have analyzed the synoptic conditions which lead to the occurrence of heatwaves in Romania, over the period 1961 – 2015. By analyzing 111 HW events they found that there are two major types of weather patterns associated with HW occurrence, namely positive or neutral sea level pressure anomalies and persistent ridges, over the analyzed region. Over the same period (i.e. 1961 – 2015), Croitoru et al. (2016) found that the frequency of heatwaves, defined based on the daily maximum temperature, shows a significant increasing trend, throughout the country. Looking at a more regional scale, Croitoru and Piticar (2013) have shown that there is an increasing trend in the frequency of heatwave events over the extra-Carpathian regions of Romania (i.e. the eastern and southern part of the country) and that the daily maximum temperature is getting more extreme compared to the daily minimum temperature. Over the eastern part of the country, Hustiu (2016) has shown that the annual frequency of heatwave events features an increasing trend over the period 1961 – 2013, while in a more recent study, Micu et al. (2021) have shown that the southern part of the Carpathian Mountains is facing a significant warming trend. All the aforementioned studies are either limited in time or are very regional (Croitoru and Piticar, 2013; Hustiu, 2016; Sfîcă et al., 2017; Spinoni et al., 2015) and they were mainly focused on the analysis of trends in the heatwave frequency. To our knowledge no in-depth analysis, for this region, has been made regarding the variability and trend for compound events (e.g. hot and dry summers). Moreover, taking into account that the frequency of extreme events (e.g. heatwaves, cold spells, drought, and floods) is projected to increase in the future (IPCC, 2021) it is imperative to also understand the physical process forcing the increase in the frequency and magnitude of these events in order to improve their predictability. Tacking into account the aforementioned limitations, the current paper is focused on two main objectives: i) to analyze the trends and the spatio-temporal variability of both hot and dry summers in Romania, as well as their combined effect (e.g. compound events) and ii) to determined the large-scale circulation patterns which trigger the occurrence of hot summers over the analyzed region, by analyzing the geopotential height conditions and the frequency of atmospheric blocking during the periods characterized by a high frequency of hot days. Our study extends over the period 1951 – 2020, making it the most extensive study, from a temporal point of view, over Romania. The paper is structured as follow: in Section 2 we give a detailed description of the data and methods used in this study; in Section 3 we show the main results of our analysis, while the main conclusions are presented in Section 4.

2 Data and methods

Globally, heatwaves are recognized either by utilizing a threshold-based methodology (Perkins and Alexander, 2013) or by using the exceedance of a fixed absolute value (e.g. daily maximum temperature > 30°C) (Robinson, 2001). In general, the method based on fixed thresholds takes into account periods of consecutive days when the daily maximum temperature (Tx) is above a certain percentile for a particular calendar day. In this study, we have used the 90th percentile, based on a 15-day window centered on each calendar day (Perkins and Alexander, 2013). For the duration, we have tested different lengths of 3, 4, 5, and 6 consecutive days (not shown), and for the current analysis we have chosen a period of 5 days. This threshold has been chosen in such a way to ensure enough heat wave events to be considered, but also to remove small events and also this is a threshold which is recommended by the Expert Team on Climate Change Detection and Indices (ETCCDI). The mean daily 90th percentile was calculated over the baseline period 1971 – 2000. The daily maximum temperature used in this study was extracted from the E-OBSv23.1e data set (Cornes et al., 2018). Here, the heatwave duration index (HWDI) is defined as the number of days per month/season when the afore-mentioned criteria were satisfied, while the number of heat waves (HW) is defined as the number of heatwaves per month/season. The temporal evolution of the HWDI for each summer month (i.e. June, July, and August) as well as for the whole summer season (JJA), for all considered lengths (i.e. 3, 4, 5 and 6 days, not shown), indicate a strong interannual variability and relatively significant decadal differences. As expected, the smaller the length of the threshold, the longer the heatwave. Globally, different duration thresholds have been employed, depending on the analyzed regions. For example, in Canada, a duration threshold ≥2 days has been used (Smoyer-Tomic et al., 2003), in Hungary and France a duration threshold ≥3 days has been considered (Rey et al., 2007), while in China and Ukraine a duration threshold ≥ 5days has been used (Chen and Li, 2017; Shevchenko et al., 2014). In the eastern part of Europe (e.g. Bulgaria), a duration threshold ≥3 days has been found useful (Gocheva et al., 2006). Since Romania is situated in the eastern part of Europe, where a threshold ≥ 5 or 6 days has been tested and because we want to analyze only extreme heatwaves in this study, the rest of the analysis is focused on a threshold ≥5 days.

The hydroclimatic conditions, with a special focus on the drouth component are defined by considering the 1- month, 3-month and 6-month Standardized Precipitation Evapotranspiration Index (SPEI) (Vicente-Serrano et al., 2010). For this analysis, we used the June, July, and August SPEI1 index and the August SPEI3 index, which integrates the drought conditions over the whole summer months (i.e. June-July-August). The SPEI index was computed based on the precipitation (PP) and the Potential Evapotranspiration (PET) data extracted from the E-OBS v23.0e data set, with a spatial resolution of 0.1° x 0.1° and a temporal resolution covering the period 1950 – 2020. The computation of SPEI is based on the probability distribution of the difference between PP and PET (PP - PET) and the data is normalized into a log-logistic probability distribution. The potential evapotranspiration data was computed by employing the Penman – Monteith equation (Vanderlinden et al., 2008). The advantage of using SPEI is that it is standardized on a given period and a predefined distribution. Therefore, each SPEI value corresponds to a predefined probability. Here, we choose the threshold of -1 meaning that all occurrences of SPEI below the threshold would be considered as drought. This threshold generally corresponds to a moderate to extreme drought event. Taking into account our definition HW and drought, a compound hot and dry (CHD) event is defined as a combined index when a heat wave episode occurs during a period of drought conditions (e.g. August SPEI3 ≤-1). This definition has also been used successfully for other regions (Geirinhas et al., 2021; Ionita et al., 2021a; Russo et al., 2019).

138 To analyze the large-scale driving mechanism of heatwaves, we use the daily temperature at 850mb level (TT850), the daily
139 geopotential height at 500mb level (Z500), the vertical integral of eastward and northward water vapor flux, as well as the
140 daily zonal and meridional wind at 500mb level. These datasets have been extracted from the ERA5 reanalysis project
141 (Hersbach et al., 2020), and have a spatial resolution of 0.25° × 0.25°, covering the 1950–2020 period. We also used two-
142 dimensional (2D) atmospheric blocking index defined by (Scherrer et al., 2006). To compute the 2-D blocking index, we have
143 used the daily geopotential height at 500mb (Z500) obtained from the ERA5 reanalysis project for the period 1950– 2020.
144 The 2-D blocking index is an extension of the one-dimensional (1-D) Tibaldi-Molteni (TM) index (Tibaldi and Molteni, 1990)
145 to a two-dimensional map of blocking frequencies at every grid point. The southern geopotential height gradient (GHGS) and
146 the northern geopotential height gradient (GHGN) for each grid point are evaluated as follows:

147 $GHGS = (Z(\phi_0) - Z(\phi_0 - 15^0))/15^0$

148 $GHGN = (Z(\phi_0 + 15^0) - Z(\phi_0))/15^0$

149 where ϕ_0 is the latitude of the considered grid point varying from 35°N to 75°N. For each month we have calculated the ratio
150 between the number of days when a certain grid point was blocked, i.e. the conditions GHGS > 0 and GHGN < (-10m/°.lat)
151 are simultaneously satisfied for at least five consecutive days.

152 The extremeness of the July 2012, August 2015 and Jun 2019 heatwaves, was analyzed by employing the ranking maps
153 methodology (Bakke et al., 2020b; Ionita et al., 2017). In this respect, we have computed the TX90 for the 70-year period
154 (1951–2020), and for each analyzed month (i.e. June, July and August), and the years were ordered from the most extreme
155 (highest temperature) to the least extreme value. A rank of 1 implies record-breaking high temperature (in the case of TX90),
156 a rank of 2 indicates that the respective month had the second most extreme value, etc.

157 The physical mechanism behind the occurrence of heatwaves was identified by computing composite maps instead of the
158 correlation maps, in order to avoid nonlinearities in the analyzed data. The composite maps were constructed for years when
159 the total area affected by a HW was higher than 20% at country level. We selected this threshold to capture the strength of
160 the climate anomalies associated with monthly HW conditions and the number of maps satisfying this criterion. The performed
161 analysis has shown that the results are not sensitive to the exact threshold value used for our composite analysis (not shown).
162 The significance of the composite maps is based on a standard t-test (confidence level 95 %). To test the spatial-temporal
163 stability of the relationship between the HWDI and the large-scale atmospheric circulation we also make use of stability maps,
164 a methodology successfully applied in the seasonal forecast of the European rivers and Arctic sea ice (Ionita et al., 2008,
165 2019) In order to detect stable predictors, the variability of the correlation between the HWDI time series and the gridded data
166 is investigated within a 31-year moving window over the period 1950 - 2020. The correlation is considered stable for those
167 regions where the HWDI index and the gridded data (i.e. Z500) are significantly correlated at the 95%, 90%, 85% or 80%
168 level for more than 80% of the 31-year moving windows. A detailed description of this methodology is given in the
169 aforementioned papers.

170 The trend analysis was performed by using the Mann-Kendall test (Mann, 1945). The Mann–Kendall test has been intensively
171 used to identify the trend in the hydrometeorological time series (Adamowski et al., 2009; Dang et al., 2020 and the references

therein). In order to identify trends of auto-correlated climatic time series we used a modified version of the Mann–Kendall test performed (Hamed and Ramachandra Rao, 1998). In the new version of the test, the significance of a trend is determined by the Z statistic that has a normal distribution with a mean of 0 and variance of 1. A positive Z value indicates an increasing trend, whereas a negative Z value shows a decreasing trend in the time series. The non-parametric Sen's slop method (Sen, 1968) was used to evaluate the magnitude of the trends.

3 Results

3.1 Summer heat waves in Romania: variability and trends

The heatwave duration index (HWDI) averaged at the country level and the fraction of the country affected by a heatwave (AREA) are shown in Figure 2. This figure reveals that there is strong interannual and decadal variability throughout all summer months (Figure 2- left column). For June, there is a statistically significant increase in both HWDI (Figure 2a and Table S1) and AREA (Figure 2b), with a much higher frequency of both after the beginning of the 1990's. The longest heatwave was recorded in June 2019 and lasted 10 days, and more than 90% of the country was affected. Until the beginning of the 1990's there were relatively few HWs, most o them observed between 1960 and 1970, but their duration was much smaller compared to the events recorded from 2000 onwards. Also, in terms of the affected area, after 1990's most of the heatwaves had a larger spatial extent, with an area covered by a HW of more than 80% in1996, 2002, 2003, 2010, 2012, and 2019, respectively.

As in the case of June, for July we observe also a statistically significant increase both in the HWDI (Figure 2c and Table S1) and the AREA (Figure 2d). At the beginning of the analyzed period (i.e. 1950 – 1960), there were heatwave events lasting on average 4 – 5 days (when averaged at country level) and covering an area up to 80%. Between 1970 and 1985 no HWs were recorded throughout the country. After 1985 there is a steep increase in the duration of the HWs, with the longest HWs in July 2007 and 2012, when the whole country was affected (i.e. AREA = 100%). Years 1987, 2002, 2007, 2012, and 2015 have been characterized by HWs with a spatial coverage of more than 80% (Figure 2d). For August, the temporal evolution of HWDI (Figure 2e) and AREA (Figure 2f) follows the same path as June and July, meaning a significantly increasing trend in both the duration and AREA (Table S1). Over the period 1964 – 1988 no HWs has been recorded in August, while most of the longest and extended HWs were recorded in the last two decades of the analyzed period. The longest HW recorded in August was in 2015, followed by 2012, 1992, and 1952. In 1992, 2012, and 2015 the area covered by HWs was higher than 90% (Figure 2f). For all analyzed months, the HWs recorded in the last two decades were both longer and had a higher spatial extent. If we analyzed the whole summer months taken together (JJA), we have a very clear picture (Figure 2g and 2h): the period 1950 – 1970 was characterized by the occurrence of HWs with a duration varying between 3 to 10 days, averaged at country level, and a spatial extent between 20% up to 80%, followed by a relatively HW free period between 1971 and 1985. After this period there was a significant increase in the duration of the HWs and most of them reached a spatial extent of more than 50%, especially over the last two decades (i.e. 2001 – 2020).

Since the number of HWs per year is small, especially in the first half of analyzed period (i.e. 1951 – 1985), we have aggregated the number of heatwaves in decades, to be able to analyze the spatio-temporal changes in their occurrence. We have performed the decadal analysis for each summer month separately (Figure S1, S2, and S3) and for the whole summer

season (JJA) as a whole (Figure 3). We focused our analysis in this way, to have an equal number of months/decade and also to provide decadal evolution of HWs hotspot, at country level. The first analyzed decade is 1951 – 1960, followed by 1961 – 1970, and so on until 2011 – 2020. Figure 3 shows that the geographical distribution of the number of HWs/decade summed over the summer months. Overall, there is an increased variability among different regions of the country depending on the analyzed decades. Over the decade 1951 – 1960 up to 24 HWs/decade have been recorded in the south-eastern part of the country (i.e. the Dobrogea region), while in the north-west part of the country up to 10 HWs/decade have been recorded (Figure 3a). Over the decade 1961 – 1970 HWs up to 8 HWs/decade have been recorded mainly in the Intra-Carpathian region (i.e. the north-west part of the country) (Figure 3b). The decade 1971 – 1980 was almost HWs free (Figure 3c), while for the decade 1981 – 1990 there were less than 2 HWs/decade at country level (Figure3d). Starting with the decade 1991 – 2000 the number of summer HWs started to increase all over the country (Figure 3e). During the 2001 – 2010 decade, the HW hotspots developed in the western part of the country and the Doborgea region (i.e. south-eastern part of the country) (Figure 3f). Over the decade 2011 – 2020, there were up to 24 HWs/decade, the most affected areas being the north-western, inside the Carpathian Chain, and the south-eastern part of the country (Figure 3g). Overall, there was up to 6 times more HWs in the last decade compared to the HWs at the beginning of the analyzed period.

When looking at the decadal distribution of HWs hotspots for each summer month separately, there are some clear differences, especially at the beginning of the analyzed period (Figure S1, S2, and S3). Over the decade 1951 – 1960, there were up to 5 HWs/decade in July (Figure S2a) and August (Figure S3a), focused in the north-western part of the country and the most south-eastern corner of the country. In June, a limited number of HWs have been recorded in this decade (~2 HWs/decade) over the eastern part of the country (Figure S1a). The decade 1961 – 1970 was characterized by up to 4 HWs/decade in June, over the north and north-western part of the country (Figure S1b), while in July (Figure S2b) and August (Figure S3b) 1 HW/decade was recorded in the western part of the country. The decade 1971 – 1980 was HW free in July (Figure S2c) and August (Figure S3c), while in June there were ~1 HW/decade over a small part of the country (Figure S1c). The decade 1981 – 1990 was characterized by up to 2HWs/decade, at country level, in July (Figure S2d) and August (Figure S3d). Starting with the 1991 – 2000 decade, the number of HWs/decade starts to increase at the country level, the most affected months being June (Figure S1e - 1g) and August (Figure S3e - 3g). Over the decade 2001 – 2010 there were up to 7 HWs/decade recorded in the south and south-eastern part of the country in June (Figure S1f), up to 6 HWs/decade in the western part of the country and the Dobrogea region, in July (Figure S2f) and up to 10 HWs/decade in August, with a focus on the Dobrogea region (Figure S3f). For the last decade (i.e. 2011 – 2020) the number of HWs/decade has increased in all months, but their spatial distribution differs. In June (Figure S1g), the highest number of HWs/decade was recorded over the north-western part of the country (up to 10 HWs/decade) and over the Doborgea region. In July, the HWs hotspots are over the northern and eastern part of the country (Figure S2g), while in August there is a homogenous distribution of up to 10HWs/decade, throughout the country (Figure S3g).

From the decadal analysis of the number of HWs, we can clearly state that the decade 2011 – 2020 was characterized by a significant increase in the number of HWs compared to the previous decade, this increase being the strongest in August. There are preferred hotspots for the HWs occurrence, depending on the analyzed decade and month, these hotspots being strongly influenced by the geographical distribution of the Carpathian Mountains. The most affected regions by the HW occurrence are the north and north-western part of the country and the Dobrogea region. Dobrogea is a region which has been subjected

244 to a significant increase in the mean air temperature and a significant decrease in the summer precipitation (Chelcea et al.,
245 2015; Prăvălie et al., 2017). Overall, there is a significant increase, of ~0.2HWs/decade in June, over most parts of the country,
246 except some small regions in the north-eastern part (Figure 4a). In July a significant increase of ~0.1 HWs/decade can be
247 observed in the northern part of the country, while for the rest of the country no significant changes have been recorded
248 (Figure 4b). In August, there is a significant increase in the number of HWs over Romania, especially over the eastern part of
249 the country (~0.2 HWs/decade) (Figure 4c). When we consider all summer months together, the increase in the number of
250 HWs is significant at the country level, with an increase of up to 0.4HWs/decade in the eastern part of the country (Figure
251 4d).

3.2 Summer droughts in Romania: variability and trends

253 To analyze the variability and trends of drought conditions, at the country level, we performed a similar analysis like in the
254 previous section: we averaged the SPEI at the country level (Figure 5), we performed the decadal analysis (Figure 6), and the
255 trend analysis (Figure 7). The temporal evolution of June SPEI1 (Figure 5a), July SPEI1 (Figure 5c), August SPEI1 (Figure
256 5e), and August SPEI3 (Figure 5g) indicates a strong interannual variability of the drought conditions, at the country level,
257 and a statistically significant drying trend for SPEI1 August. For June, the driest years, both in terms of amplitude (Figure 5a)
258 and spatial coverage (AREA, Figure 5b) were: 1950, 1968, 2003, 2006 and 2012. For July, the driest years were: 1952, 2007,
259 2012, and 2015 (Figure 5c), respectively. For these years, the drought conditions extended to more than 60% of the country
260 (Figure 5d). In August, the driest years, at the country level were recorded in 1952, 1992, 2000, 2003 and 2018 (Figure 5e),
261 with the drought conditions covering more than 60% of the country (Figure 5f). Moreover, in the case of August SPEI1 only
262 negative values have been recorded for 13 consecutive years, from 2008 until 2020. August SPEI3, which is an indicator of
263 drought conditions over the whole summer, indicates that the driest summers, over Romania, were: 1950, 1952, 2000, 2003,
264 2012, 2015 and 2018, respectively (Figure 5g). For all these summers, drought affected more than 70% of the country (Figure
265 5h).

266 The drought hotspots, at a decadal scale (Figure 6), indicate strong spatio-temporal variability between the different analyzed
267 decades and between different regions of the country. Over the 1951 – 1960 decade (Figure 6a), the drought hotspots (defined
268 as the number of months/decade when August SPEI3 ≤-1 for each grid point) was focused in the north-eastern part of the
269 country. For this period, there were up to 3 summers/decade characterized by drought conditions over these regions. For the
270 decade 1961 – 1970 (Figure 6b) there was a relatively limited number of dry summers (~2 dry summers/decade) throughout
271 the country, mostly focused on the north-western part and south part of the country, while the decade 1971 – 1980 (Figure
272 6c) was drought free. For the decade 1981 – 1990 (Figure 6d), there is a rather homogenous pattern at the country level, with
273 up to 2(1) dry summers/decade affecting the western (eastern) part of the country. The decade 1991 – 2000 (Figure 6e)
274 indicates also a rather homogenous pattern of the drought conditions at country level, with up to 4 dry summers/decade in the
275 western part of the country and 3 dry summers/decade over the rest of the country. The decade 2001 – 2010 is characterized
276 by an west-east gradient in the drought conditions, with the highest number of dry years (~4) in the south-eastern part of the
277 country (Figure 6f). Over the 2011 – 2020 decade, the drought hotspots are located mainly over the western part and the south-
278 eastern part of the country (Figure 6g). The highest number of dry summers/decade were record throughout this decade (i.e.
279 2011 – 2020), with up to 6 dry summers/decade over the whole western part of the country and over the south-eastern part.

280 Overall, the decadal spatio-temporal evolution of the drought conditions (Figure 6) indicates that drought events are not
281 homogenous throughout the country and that the decades with the highest number of dry summers were 1991 – 2000, 2001 -
282 2010 and 2011 – 2020, respectively. A similar pattern is observed when looking at the SPEI trends, both at monthly (Figure
283 7a-c) and seasonal time scale (Figure 7d). Overall, in June there is a non-significant drying trend over the north-western and
284 south-eastern parts of the country (Figure 7a and Table S2). In July there is an overall non-significant drying trend over the
285 south-western and south-eastern parts of the country (Figure 7b), while in August, the spatial trend pattern is rather distinct
286 compared to June and July, being characterized by a general drying trend at country level, but significant only over the eastern
287 part of the country (Figure 7c). August SPEI3 trend, which takes into account all summer months, it's a combination of the
288 features identified for each month analyzed separately: a drying trend over the whole country, but statistically significant only
289 over the south-eastern part of the country (i.e. Dobrogea region) (Figure 7d).

290 **3.3 Historical evolution of compound events (e.g. warm and dry summers) in Romania**

291 In this sub-section, we analyze the co-variability between hot and dry summers in terms of lagged and in phase spatial
292 correlation maps between the monthly /seasonal HWDI and monthly SPEI (Figure 8) and conditional probability maps (Figure
293 9). The lagged correlation maps (SPEI leading) have been computed and analyzed in order to test for possible influence of
294 the pre-conditions of dry springs/early summer on the occurrence of summer heat waves. To find the best combination, in
295 terms of compatible months for both hot and dry events, we have computed the spatial correlation maps between the monthly
296 SPEI with the monthly HWDI with different time-lags (e.g. SPEI leading). For example, June HWDI was correlated with
297 April SPEI1, SPEI3 and SPEI6 (not shown), May SPEI1, SPEI3 and SPEI6 (not shown) and June SPEI1 (Figure 8a), SPEI3
298 (not shown) and SPEI6 (not shown). The highest correlations, both in terms of amplitude and spatial extent have been obtained
299 for the combination June HWDI and June SPEI1 (Figure 8a). This finding is confirmed also by looking at the correlation
300 coefficient, both with lag and in phase, between the HWDI index averaged at country level (i.e. the time series in Figure 2a)
301 and different combination the monthly SPEI averaged at country level (Figure S4). Also, for the country-averaged time-series,
302 the highest correlation was obtained for June HWDI and June SPEI1. In terms of spatial extent, the highest correlations (e.g.
303 ~0.5) have been obtained for the western and southern part of the country (Figure 8a). Nevertheless, a significant correlation
304 between HWDI and SPEI over these regions, does not necessarily imply that each drought will always co-occur with a
305 heatwave over that region or vice-versa. The conditional probability map for June, which implies the probability of co-
306 occurrence of both a dry (June SPEI ≤ -1) and a hot (June HW >1) month, indicates the most prone regions of a combined hot
307 and dry June are the areas located in the eastern part of the country (Figure 9a). For July, the highest correlation has been
308 found also for the in-phase relationship (i.e. July HW and July SPEI1) (Figure 8b). Compared to June, in July the spatial
309 correlations between July HW and July SPEI1 are significant all over the country, with the highest amplitudes over the extra-
310 Carpathian regions and over small areas in the north-western part. This dipole-like structure clearly emphasizes the influence
311 of the Carpathian Mountains on the climate variability of Romania, which is in agreement with previous studies over this
312 regions which have shown that the Carpathian mountains plays a significant role in the hydroclimatic variability of the country
313 (Busuioc et al., 2015; Ionita, 2015). In terms of co-variability, the most prone regions for a combined hot and dry July are, as
314 in the case of June, the areas located in the eastern part of the country (Figure 9b). In August, the highest correlations, both
315 based on the amplitude but also from a spatial extent, have been found between August HWs and August SPEI3 (Figure 8c
316 and S4). The correlations between August HWs and August SPEI3 reached values up to -0.7 almost for the whole country,

with small exceptions in the south-eastern corner of the country. The occurrence of HWs in August seems to be influenced not only by the hydroclimatic conditions in August, but also from the previous months. The conditional probability map (Figure 9c) indicates that hot and dry events have a higher probability of occurrence compared to June and July and the risk of hot and dry events is distributed all over the country, with small exceptions in the mountains areas (i.e. Apuseni Mountains and Retezat Mountains). When we look at the whole summer months together, the highest correlations are obtained between JJA HWs and August SPEI3. The spatial correlation map between JJA HWs and August SPEI3, reaches values up to ~-0.8 for almost the entire country (Figure 8d) and a value of -0.71 when we averaged at country level (Figure S4). In terms of co-variability, the most prone regions for combined hot and dry summers, are the areas located in the eastern part of the country (Figure 9d). When considering the 1 month lag, there are still some regions showing significant negative correlations between SPEI and HW, mainly for July HW and June SPEI1 over the southern part of the country, and August HW and July SPEII1 over the western part of the country (not shown). Although the lagged correlations are smaller in amplitude compared to the in-phase correlations, the lagged relationship indicates that there might be some influence of the drought conditions on the heatwaves in the upcoming months, especially in the case of July and August HWs.

3.4 Extreme heatwave events in Romania and their driving factors

The analysis of the temporal variability of the HWDI and AREA (Figure 2) has emphasized some extreme HWs for each analyzed month, both in terms of duration and spatial coverage. Thus, in this sub-section, we make a detailed analysis for the longest HW for each month, in terms of extremeness (e.g. rank maps) and large-scale driving factors. The analysis is focused on three distinct cases: July 2012, August 2015, and June 2019, respectively.

July 2012 was marked by persistent heat waves, which have determined extremely high temperatures at the beginning of the month in the western part of the country, afterwards extending to all regions, but especially in the plain and plateau areas (Figure 10a). In some regions of the country (e.g. eastern and central part) the duration of the HWs was up to 24 days. In terms of drought, most of the country was affected by moderate to extreme drought in July 2012 (Figure 10b), with small exceptions in the north-western part of the country. July 2012, was the hottest month on record (e.g. over the period 1950 – 2020) over most of the country (Figure 10c). In July 2012, 114 meteorological stations through the country recorded temperatures above 35°C (Dima et al., 2016). Over the central part of the country, from the south to the north, July 2012 was both hot and dry (Figure 10d). The peak of the heatwaves was recorded in the first week of the month (Figure S5). Starting with the 2nd of July, the atmospheric circulation was characterized by a north-easterly flow, which led to an advection of warm air masses, generated over Russia (Figure S6). At the country level, this large-scale atmospheric pattern resulted in the establishment of an excessive thermal regime and an increase in the number of hot days (i.e. daily temperatures > 35°C), especially in the southern and eastern regions (Figure 10e and S5). Between the 7th and 9th of July 2012, the daily maximum temperature up to 10°C was higher, compared to climatology, especially in the eastern part of the country (Figure S5f – S5h). These excessive temperatures were driven by the persistence of a high-pressure system over the eastern part of Romania and the presence of an atmospheric blocking center over Fennoscandia and the western part of Russia (contour lines in Figure S6).

The heat wave and drought event observed throughout the summer of 2015, affected a large portion of continental Europe and was one of the most severe dry and hot summers over the observational period (Ionita et al., 2017; Laaha et al., 2017; Van Lanen et al., 2016). Record high temperatures were observed throughout the whole summer over different parts of Europe.

Extremely high temperatures already started to be recorded in June 2015 over the Iberian Peninsula, central and eastern France, the western Alps, and Ukraine. The heatwave and drought conditions extended towards the central part of Europe in July 2015 (Ionita et al., 2017). By August 2015, the heat wave moved and continued to develop in central and eastern Europe, including Romania. For most of the month of August 2015, Romania was under the influence of extremely high temperatures. The first heat waves occurred between the 3rd and 16th of June (not shown). Between the 17th and 23rd of August, a short relief was observed, with temperatures below the climatological mean (not shown). The second and most intense heat waves (e.g. in terms of the temperature anomalies) started to develop on the 24th of August reaching it's peak at the end of the month (Figure S7). The longest heat wave was recorded over the northern and eastern parts of the country (Figure 11a). In some regions in the eastern part of the country, there were up to 24 days which fulfilled the HW definition. Overall, the drought conditions in August 2015, were not as intense as in July 2012. Only the northern part of the country experienced both heat wave and drought at the same time (Figure 11b and 11d). August 2015, was also the hottest month on record (e.g. over the period 1950 – 2020) in the northern and north-eastern part of the country (Figure 11c). The extremely high temperatures recorded, especially in the last week of August 2015 were mainly driven by the prevailing large-scale circulation. The two long-lasting heatwaves in August 2015 were determined by the extension of the North African ridge over most of the European continent (Figure 11e and Figure S8). During the peak of the second heatwave (i.e. 28.08 – 31.08.2015) the eastern part of Europe was affected by a persistent atmospheric blocking system (contour lines in Figure S8), which was centered over Romania and by positive values of the water vapor flux divergence (not shown). The anomalous Z500 center over the eastern part of Europe (Figure 11e and S8) and the divergent water vapor flux over Romania, suggests a dominant subsidence and adiabatic warming, reduced cloudiness, and increased incoming solar radiation, thus leading to excessive temperatures over the affected regions.

For the month of June, the longest and largest (in terms of spatial extent) HW event was recorded in June 2019 (Figure 2e – 2f). According to Copernicus (https://climate.copernicus.eu/surface-air-temperature-june-2019) June 2019 was the hottest June on record both globally and for Europe, with the central and eastern Europe particularly warm throughout the whole month. In June 2019, the north-western and south-eastern parts of Romania were the most affected regions by extreme temperatures (Figure 12a and 12c). Record breaking temperatures were recorded in the most northern part of the country as well as in the Dobrogea region (Figure 12c). These record breaking temperatures were corroborated with drought conditions (Figure 12b and 12d). The eastern, central, and south-western parts of the country were less affected by extreme temperatures (Figure 12a and 12c) and these regions were characterized by wet conditions throughout the month (Figure 12b). The particular spatial pattern was mainly influenced by the spatial pattern of the large-scale atmospheric circulation (Figure 12e). The atmospheric circulation at the peak of the heatwave event (Figure S9 and S10) was characterized by a persistent wave-like pattern extending from the North Atlantic Ocean towards Eurasia (Figure 12e and S10). Positive (negative) geopotential anomalies were observed over eastern Europe (central North Atlantic and central Siberia) corresponding to the local positive (negative) temperature anomalies underneath (Figure 12e and S9)). The spatial structure of the Z500 field resembles the classic omega blocking circulation (Figure S10 - contour lines). This pattern favors the advection of warm air from the Sahel towards the eastern part of Europe and enhances the incoming solar radiation, leading to extremely high temperature anomalies underneath the high-pressure system.

389 All analyzed extreme HWs in this section were mainly driven by the presence of a high-pressure system over the analyzed
390 region, during the peak of the HW event. In order to identify if the presence of a persistent high-pressure system is a necessary
391 ingredient for all HWs identified throughout the period 1950 – 2020, we have computed the composite maps for the years
392 when the HWDI index (Figure 2 – left column) was >5 days and the corresponding Z500 anomalies and the corresponding
393 wind vectors. We performed the analysis for each month separately (Figure 13). Due to the fact that the relationship between
394 the large-scale atmospheric circulation and the European hydroclimate was found to be limited due to non-stationarity issues
395 (Ionita et al., 2020; Rimbu et al., 2004; Vicente-Serrano and López-Moreno, 2008), we have computed also the stability maps
396 between the HWDI and the monthly Z500. The aim of the composite map analysis is to analyze the relationship between the
397 HWDI and the large-scale atmospheric patterns, but this methodology does not consider if the relationship between the two
398 variables is stationary in time or not. In order to overcome the problem of non-stationarity and to test if the identified
399 relationship between the HDWI and Z500 is stable over time, we employed a methodology, namely the stability maps, used
400 for the monthly to seasonal prediction of the mean runoff of the Elbe River and in dendroclimatological studies (Ionita et al.,
401 2015; Nagavciuc et al., 2019).

402 The June composite map of Z500 anomalies and the corresponding wind vectors for years with HWs lasting more than 5 days,
403 is characterized by positive Z500 anomalies over the central and eastern part of Europe and negative Z500 anomalies over the
404 central North Atlantic Ocean (Figure 13a). Moreover, HWs in June, in Romania, are also associated with an increase in the
405 number of atmospheric blocking days, centered over the south-eastern part of Europe (Figure S14a). The spatial structure of
406 the Z500 anomalies, centered over the eastern part of Europe, leads to the advection of hot and dry air from the north-eastern
407 part of Europe. The large-scale atmospheric circulation associated with HWs over Romania, in July, is similar with the spatial
408 structure identified in June, both in the Z500 field (Figure S13b) as well as in the case of 2D atmospheric blocking (Figure
409 S14b). In August, the spatial structure of the Z500 field, associated with the occurrence of HWs over Romania, is characterized
410 by a wave-train like pattern of alternating Z500 anomalies, which extends from the eastern part of the U.S until Eurasia (Figure
411 S13c). Extreme HWs, in August, are associated with a low pressure system over the eastern part of the U.S., followed by
412 positive Z500 anomalies over the western part of the central North Atlantic Ocean, negative Z500 anomalies centered over
413 the British Isles, and positive Z500 anomalies over the central and eastern parts of Europe. This wave-like pattern suggests a
414 stationary Rossby wave pattern, which is usually associated with heatwaves and droughts over the Eurasian continent (Bakke
415 et al., 2020a; Barriopedro et al., 2011; Ionita et al., 2012; Schubert et al., 2014). As in the case of June and July, HWs in
416 August are also associated with an increased frequency of atmospheric blocking over the eastern part of Europe (Figure S14c).
417 The significant relationship between the HWDI and Z500 obtained via de composite map analysis is also confirmed by the
418 stability maps. June HWDI is stably and positively correlated with June Z500 over the eastern part of Europe, centered over
419 Romania (Figure 15a). The same pattern can be observed also when we compute the stability map between July HWDI and
420 July Z500 (Figure 15c). In the case of August, the HWDI is stable and positively correlated with Z500 over a region extended
421 from the North Atlantic basin towards central and eastern part of Europe and negatively correlated with Z500 centered over
422 the British Isles and North Sea (Figure 15e). This dipole-structure is reminiscent of the East Atlantic teleconnection pattern,
423 which was found to have a significant influence on the variability of temperature and precipitation over Europe, throughout
424 the whole year (Gao et al., 2017). Based on the monthly stability maps identified in Figure 15, we defined a Z500 index
425 averaged over the stable regions (black squares in Figures 15a, 15c, and 15e) to analyze the interannual variability of the Z500

over these regions in a long-term context. This analysis was motivated by the fact that it has been suggested that the Z500 over central and western part of Europe has increased recently leading to an increase in the frequency of HWs over these regions (Porebska and Zdunek, 2013; Tomczyk and Bednorz, 2016). June Z500 index exhibits strong interannual variability over the last 70 years, with the highest amplitudes since the beginning of 1990s (Figure 15b). Notably, the highest value of this index was recorded in 2019, which is also the month with the longest June heatwave (Figure 2a). Over the period 1990 – 2020 there is a significant increasing trend in the June Z500 averaged over the eastern part of Europe, a trend which closely resembles the one observed for the June HWDI (Figure 2a). The results of the trend analysis for each month and each analyzed period are given in Table S3. As in the case of June, July Z500 index exhibits also strong interannual variability over the last 70 years and a significant increasing trend over since 1990's onward (Figure 15d). The highest values of this index were recorded in 1954,1987, 1988, 2007, 2012 and 2015, respectively. July 2012 is also the month with the longest July heatwave over the analyzed period (Figure 2c). The time series of August Z500 index exhibits also strong interannual variability over the last 70 years and a significant increasing trend over the period 1990 - 2020 (Figure 15f). The highest value of this index was recorded in 1952, 1962, 1992, 2010, 2015, 2017 and 2019, respectively. August 2015 is also the month with the longest August heatwave (Figure 2c). Overall, the time series of the monthly Z500 presents a strong interannual variability and a significantly increasing trend starting with the beginning of the 1990's, which mirrors the trends observed in the monthly HWDI (Figure 2). For July and August, the trend of the Z500 indices is significant for both analyzed periods (i.e. 1950 – 2020 and 1990 – 2020), while for June the trend is significant only when we consider the 1990 – 2020 period (Table S3).

4 Conclusions

The main findings of this study indicate that the regional extreme temperature over Romania are following the same path as the ones observed at continental and global scale, namely the summer temperature extremes have become more frequent and their amplitude has increased, especially over the last two decades. The increase in the frequency and magnitude of summer temperature extremes, over Romania, has been occurring at the same time with an overall drying trend, especially over the eastern part of the country. However, the changes in the HWs over Romania present also a decadal/multidecadal component, which is in agreement with previous studies at European level as well at more regional spatial scales, which have shown that the summer temperature is strongly influenced by the Atlantic Multidecadal Oscillation (Della-Marta et al., 2007; Ionita et al., 2013). The tempeoral evolution of the HWDI time series can be regarded as a combination between multi-decadal variability and anthropogenic induced climate change.

The length, spatial extent and frequency of HWs in Romania has increased significantly over the last 70 years, for all summer months, with an increase of the heat wave duration of ~0.52 days/decade (in June), ~0.31 days/decade (in July) and ~0.43 days/decade (in August). After the 1990's the rate of increase in the frequency, length and spatial extent has significantly accelerated, reaching unprecedented length and spatial extent after 2000 until the end of the analyzed period. Overall, the most active decades, in terms of HWs, were 1951 - 1960, 2001 – 2010 and 2011 – 2020, while the longest and most extensive (in term of spatial extent) HWs were observed in July 2012, August 2015 and June 2019. Over the decade 2021 -2020 there were up to 24 HWs record thoughts the summer season. In terms of drought variability and trends, significant changes in the drought conditions (i.e. significant drying trend) have been observed over the eastern part of the country in August for SPEI3 and July for SPEI1 and the driest decade has been over the period 2011 – 2020.

The strongest correlation between hot and dry events has been observed for an "in-phase" relationship, indicating that for our analyzed region the soil-moisture memory does not play a significant role in the occurrence of heat waves throughout the summer months. Overall, there is an increase probability of co-occurrence of hot and dry events in the half eastern part of the country, especially in June and July. Although the significant correlation between SPEI and extreme temperatures throughout concurrent month does not provide any information about the effect of antecedent drying on the occurrence of HWs, thus it does not have a predictive skill, it does indicate a strong land-atmosphere coupling over the analyzed region. A lagged-relationship has been observed only for 1-month lag (SPEI leading) over the southern (in July) and western part of the country (in August). This is in agreement with recent studies (Stegehuis et al., 2021), which have shown that the antecedent soil moisture has a significant influence on the summer HWs especially over the western part of Europe, whereas over the eastern part of Europe the large-scale drivers explain the occurrence of extreme temperatures. The strongest changes, in terms of frequency and amplitude of hot and dry summers, were observed in the extra-Carpathian Mountain regions (e.g. south and south-eastern part of Romania), mainly because the Carpathian Mountains act as a barrier for the Atlantic air masses, limiting their oceanic influences to the western and central part of the country, which experience on average milder summers and heavier rainfalls, while the eastern part of the country is prone to rainfall deficit and higher temperatures, due to advection of hot and dry air either from the east or from the south.

The occurrence of HWs in Romania has been related to anticyclonic conditions and a higher frequency of blocking situations corroborated with daily maximum temperature anomalies up to 10°C and with water vapor flux divergence, which showed a positive anomalous signals during hot and dry events. This is in agreement with previous study for other regions (e.g. western part of Europe) which have shown that HWs tend to occur under the influence of anticyclonic circulation, which is conductive to and intensification of the radiation flux and cloudless weather (Porebska and Zdunek, 2013; Tomczyk et al., 2017; Tomczyk and Bednorz, 2016). The occurrence of HWs over the analyzed region is stably correlated with the geopotential height centered over Romania and in the neighboring regions. The geopotential height shows also an increase amplitude after the beginning of the 1990's, which follows the same temporal variability as the HWDI index and the AREA index, thus supporting the finding that the increase in the number of HWs over the last 2 decades could be explained, at least partially, by the increase in the regional geopotential height. Similar results have been found also for the central and western part of Europe (Porebska and Zdunek, 2013; Tomczyk and Bednorz, 2016). In their study, Porebska and Zdunek (2013), have shown that heat waves over central part of Europe were often associated with an increased frequency of blocking situations over the Atlantic Ocean and Eastern Europe. Similar results have been found by Tomczyk and Bednorz (2016), which have shown that the occurrence of HWs in the central part of Europe, was mainly driven with positive anomalies of the Z500 over the analyzed region. Thus, a possible explanation regarding the increase in the frequency of HWs in Romania, over the past two decades, might be related to more frequent blocking situations and an increase in the geopotential height over the analyzed region.

Finally, we conclude that the analysis of both hot and dry events in connection with the large-scale atmospheric drivers provides an useful tool in order to find plausible physical mechanism which can explain the changes in the frequency and amplitude of these extreme events. Our findings are in line with the recently published IPPC report (IPCC, 2021), which states that there is an overall global increase in the frequency of heatwaves. Thus, our analysis of the variability and changes of heatwaves and droughts and their combined effect could be used to improve the adaptation strategies to extreme events and to improve the resilience plans at country level.

References

499

Adamowski, K., Prokoph, A. and Adamowski, J.: Development of a new method of wavelet aided trend detection and estimation, Hydrol. Process., 23(18), 2686–2696, doi:https://doi.org/10.1002/hyp.7260, 2009.

Bădăluță, C.-A., Perșoiu, A., Ionita, M., Nagavciuc, V. and Bistricean, P.-I.: Stable H and O isotope-based investigation of moisture sources and their role in river and groundwater recharge in the NE Carpathian Mountains, East-Central Europe, Isot. Environ. Heal. Stud., 55(2), 1–18, doi:https://doi.org/10.1080/10256016.2019.1588895, 2019.

Bakke, S. J., Ionita, M. and Tallaksen, L. M.: The 2018 northern European hydrological drought and its drivers in a historical perspective, Hydrol. Earth Syst. Sci., 24, 5621–5653, doi:10.5194/hess-2020-239, 2020a.

Bakke, S. J., Ionita, M. and Tallaksen, L. M.: The 2018 northern European hydrological drought and its drivers in a historical perspective, Hydrol. Earth Syst. Sci., 24(11), 5621–5653, doi:10.5194/hess-24-5621-2020, 2020b.

Balting, D. F., AghaKouchak, A., Lohmann, G. and Ionita, M.: Northern Hemisphere drought risk in a warming climate, npj Clim. Atmos. Sci., 4(1), 61, doi:10.1038/s41612-021-00218-2, 2021.

Barriopedro, D., Fiscer, E. M., Luterbacher, J., Trigo, R. M. and García-Herrera, R.: The Hot Summer of 2010 : Map of Europe, Science (80-.)., 332(April), 220–224, doi:10.1080/10255842.2015.1069566, 2011.

Busuioc, A., Caian, M., Cheval, S., Bojariu, R., Boroneant, C., Baciu, M. and Dumitrescu, A.: Variabilitatea și schimbarea climei în România., 2010.

Busuioc, A., Dobrinescu, A., Birsan, M. V., Dumitrescu, A. and Orzan, A.: Spatial and temporal variability of climate extremes in Romania and associated large-scale mechanisms, Int. J. Climatol., 35(7), 1278–1300, doi:10.1002/joc.4054, 2015.

Chelcea, S., Ionita, M. and Adler, M.-J.: Identification of dry periods in the dobrogea region, IGI Global., 2015.

Chen, Y. and Li, Y.: An Inter-comparison of Three Heat Wave Types in China during 1961-2010: Observed Basic Features and Linear Trends, Sci. Rep., 7(April 2016), 2–11, doi:10.1038/srep45619, 2017.

Christidis, N., Jones, G. S. and Stott, P. A.: Dramatically increasing chance of extremely hot summers since the 2003 European heatwave, Nat. Clim. Chang., 5(1), 46–50, doi:10.1038/nclimate2468, 2015.

Cornes, R. C., Schrier, G. Van Der, Besselaar, E. J. M. Van Den and Jones, P. D.: An Ensemble Version of the E-OBS Temperature and Precipitation Datasets, Geophys. Res. Atom, 123, doi:10.1029/2017JD028200, 2018.

Croitoru, A.-E., Piticar, A., Ciupertea, A.-F. and Roșca, C. F.: Changes in heat waves indices in Romania over the period 1961–2015, Glob. Planet. Change, 146, 109–121, doi:https://doi.org/10.1016/j.gloplacha.2016.08.016, 2016a.

Croitoru, A. E. and Piticar, A.: Changes in daily extreme temperatures in the extra-Carpathians regions of Romania, Int. J. Climatol., 33(8), 1987–2001, doi:10.1002/joc.3567, 2013.

Croitoru, A. E., Piticar, A., Ciupertea, A. F. and Roșca, C. F.: Changes in heat waves indices in Romania over the period 1961–2015, Glob. Planet. Change, 146, 109–121, doi:10.1016/j.gloplacha.2016.08.016, 2016b.

Dang, V. H., Tran, D. D., Cham, D. D., Hang, P. T. T., Nguyen, H. T., Truong, H. Van, Tran, P. H., Duong, M. B., Nguyen, N. T., Le, K. Van, Pham, T. B. T. and Nguyen, A. H.: Assessment of Rainfall Distributions and Characteristics in Coastal Provinces of the Vietnamese Mekong Delta under Climate Change and ENSO Processes, Water, 12(6), doi:10.3390/w12061555, 2020.

Della-Marta, P. M., Luterbacher, J., von Weissenfluh, H., Xoplaki, E., Brunet, M. and Wanner, H.: Summer heat waves over western Europe 1880-2003, their relationship to large-scale forcings and predictability, Clim. Dyn., doi:10.1007/s00382-007-0233-1, 2007.

538   Dima, V., Georgescu, F., Irimescu, A. and Mihailescu, D.: Valuri de caldura in Romania, Editura PRINTECH., 2016.

539   Feng, S., Wu, X., Hao, Z., Hao, Y., Zhang, X. and Hao, F.: A database for characteristics and variations of global compound
540   dry and hot events, Weather Clim. Extrem., 30, 100299, doi:https://doi.org/10.1016/j.wace.2020.100299, 2020.

541   Fioravanti, G., Piervitali, E. and Desiato, F.: Recent changes of temperature extremes over Italy: an index-based analysis,
542   Theor. Appl. Climatol., 123(3), 473–486, doi:10.1007/s00704-014-1362-1, 2016.

543   Gao, T., Yu, J. and Paek, H.: Impacts of four northern-hemisphere teleconnection patterns on atmospheric circulations over
544   Eurasia and the Pacific, Theor. Appl. Climatol., 129(3), 815–831, doi:10.1007/s00704-016-1801-2, 2017.

545   Geirinhas, J. L., Russo, A., Libonati, R., Sousa, P. M., Miralles, D. G. and Trigo, R. M.: Recent increasing frequency of
546   compound summer drought and heatwaves in Southeast Brazil, Environ. Res. Lett., 16(3), 034036, doi:10.1088/1748-
547   9326/abe0eb, 2021.

548   Gocheva, A., Trifonova, L., Marinova, T. and Bocheva, L.: Extreme Hot Spells and Heat Waves on the Territory of
549   Bulgaria, ResearchGate [online] Available from:
550   https://www.researchgate.net/publication/240615319_Extreme_Hot_Spells_and_Heat_Waves_on_the_Territory_of_Bulgari
551   a, 2006.

552   Grams, C. M., Binder, H., Pfahl, S., Piaget, N. and Wernli, H.: Atmospheric processes triggering the central European
553   floods in June 2013, Nat. Hazards Earth Syst. Sci., 14(7), 1691–1702, doi:10.5194/nhess-14-1691-2014, 2014.

554   Hamed, K. H. and Ramachandra Rao, A.: A modified Mann-Kendall trend test for autocorrelated data, J. Hydrol., 204(1),
555   182–196, doi:https://doi.org/10.1016/S0022-1694(97)00125-X, 1998.

556   Hersbach, H., Bell, B., Berrisford, P., Hirahara, S., Horányi, A., Muñoz-Sabater, J., Nicolas, J., Peubey, C., Radu, R.,
557   Schepers, D., Simmons, A., Soci, C., Abdalla, S., Abellan, X., Balsamo, G., Bechtold, P., Biavati, G., Bidlot, J., Bonavita,
558   M., De Chiara, G., Dahlgren, P., Dee, D., Diamantakis, M., Dragani, R., Flemming, J., Forbes, R., Fuentes, M., Geer, A.,
559   Haimberger, L., Healy, S., Hogan, R. J., Hólm, E., Janisková, M., Keeley, S., Laloyaux, P., Lopez, P., Lupu, C., Radnoti,
560   G., de Rosnay, P., Rozum, I., Vamborg, F., Villaume, S. and Thépaut, J.-N.: The ERA5 global reanalysis, Q. J. R. Meteorol.
561   Soc., 146(730), 1999–2049, doi:https://doi.org/10.1002/qj.3803, 2020.

562   Horton, D. E., Johnson, N. C., Singh, D., Swain, D. L., Rajaratnam, B. and Diffenbaugh, N. S.: Contribution of changes in
563   atmospheric circulation patterns to extreme temperature trends, Nature, 522(7557), 465–469, doi:10.1038/nature14550,
564   2015.

565   Hustiu, M. C.: Cold and heat waves in the Barlad Plateau between 1961 and 2013, Riscuri si Catastr., 18, 31–42, 2016.

566   Ionita, M.: Interannual summer streamflow variability over Romania and its connection to large-scale atmospheric
567   circulation, Int. J. Climatol., 35(14), 4186–4196, doi:10.1002/joc.4278, 2015.

568   Ionita, M., Lohmann, G. and Rimbu, N.: Prediction of spring Elbe discharge Based on stable teleconnections with winter
569   global temperature and precipitation, J. Clim., 21(23), 6215–6226, doi:10.1175/2008JCLI2248.1, 2008.

570   Ionita, M., Lohmann, G., Rimbu, N., Chelcea, S. and Dima, M.: Interannual to decadal summer drought variability over
571   Europe and its relationship to global sea surface temperature, Clim. Dyn., 38(1–2), 363–377, doi:10.1007/s00382-011-1028-
572   y, 2012.

573   Ionita, M., Rimbu, N., Chelcea, S. and Patrut, S.: Multidecadal variability of summer temperature over Romania and its
574   relation with Atlantic Multidecadal Oscillation, Theor. Appl. Climatol., 113(1–2), 305–315, doi:10.1007/s00704-012-0786-
575   8, 2013.

576   Ionita, M., Dima, M., Lohmann, G., Scholz, P. and Rimbu, N.: Predicting the June 2013 European Flooding Based on
577   Precipitation, Soil Moisture, and Sea Level Pressure, J. Hydrometeorol., 16(2), 598–614, doi:10.1175/JHM-D-14-0156.1,
578   2015.

Ionita, M., Tallaksen, L. M., Kingston, D. G., Stagge, J. H., Laaha, G., Van Lanen, H. A. J., Scholz, P., Chelcea, S. M., Haslinger, K., Lanen, H. A. J. Van, Chelcea, S. M., Haslinger, K., Scholz, P., Chelcea, S. M. and Haslinger, K.: The European 2015 drought from a climatological perspective, Hydrol. Earth Syst. Sci., 21, 1397–1419, doi:doi:10.5194/hess-21-1397-2017, 2017.

Ionita, M., Grosfeld, K., Scholz, P., Treffeisen, R. and Lohmann, G.: September Arctic sea ice minimum prediction – a skillful new statistical approach, Earth Syst. Dyn., 10(1), 189–203, doi:10.5194/esd-10-189-2019, 2019.

Ionita, M., Nagavciuc, V., Kumar, R. and Rakovec, O.: On the curious case of the recent decade, mid-spring precipitation deficit in central Europe, npj Clim. Atmos. Sci., 3(1), 49, doi:10.1038/s41612-020-00153-8, 2020.

Ionita, M., Caldarescu, D. E. and Nagavciuc, V.: Compound Hot and Dry Events in Europe: Variability and Large-Scale Drivers, Front. Clim., 3, 58, doi:10.3389/fclim.2021.688991, 2021a.

Ionita, M., Dima, M., Nagavciuc, V., Scholz, P. and Lohmann, G.: Past megadroughts in central Europe were longer, more severe and less warm than modern droughts, Commun. Earth Environ., 2(1), 61, doi:10.1038/s43247-021-00130-w, 2021b.

IPCC: Climate Change 2021: The Physical Science Basis. Contribution of Working Group I to the Sixth Assessment Report of the Intergovernmental Panel on Climate Change, edited by V. Masson-Delmotte, P. Zhai, A. Pirani, S. L. Connors, C. Péan, S. Berger, N. Caud, Y. Chen, L. Goldfarb, M. I. Gomis, M. Huang, K. Leitzell, E. Lonnoy, J. B. R. Matthews, T. K. Maycock, T. Waterfield, O. Yelekçi, R. Yu, and B. Zhou, Cambridge University Press. In Press., 2021.

Jeong, D. Il, Yu, B. and Cannon, A. J.: Links between atmospheric blocking and North American winter cold spells in two generations of Canadian Earth System Model large ensembles, Clim. Dyn., 57(7), 2217–2231, doi:10.1007/s00382-021-05801-0, 2021.

Kautz, L.-A., Martius, O., Pfahl, S., Pinto, J. G., Ramos, A. M., Sousa, P. M. and Woollings, T.: Atmospheric Blocking and Weather Extremes over the Euro-Atlantic Sector -- A Review, Weather Clim. Dyn. Discuss., 2021, 1–43, doi:10.5194/wcd-2021-56, 2021.

Kingston, D. G., Lawler, D. M. and McGregor, G. R.: Linkages between atmospheric circulation, climate and streamflow in the northern North Atlantic: research prospects, Prog. Phys. Geogr., 30(2), 143–174, doi:10.1191/0309133306pp471ra, 2006.

Kingston, D. G., Stagge, J. H., Tallaksen, L. M. and Hannah, D. M.: European-Scale Drought : Understanding Connections between Atmospheric Circulation and Meteorological Drought Indices, J. Clim., 28(2), 505–516, doi:10.1175/JCLI-D-14-00001.1, 2015.

Kong, Q., Guerreiro, S. B., Blenkinsop, S., Li, X.-F. and Fowler, H. J.: Increases in summertime concurrent drought and heatwave in Eastern China, Weather Clim. Extrem., 28, 100242, doi:https://doi.org/10.1016/j.wace.2019.100242, 2020.

Laaha, G., Gauster, T., Tallaksen, L. M. L. M., Vidal, J.-P. J. P., Stahl, K., Prudhomme, C., Heudorfer, B., Vlnas, R., Ionita, M., Van Lanen, H. A. J. H. A. J., Adler, M. J. M.-J., Caillouet, L., Delus, C., Fendekova, M., Gailliez, S., Hannaford, J., Kingston, D., Van Loon, A. F. A. F., Mediero, L., Osuch, M., Romanowicz, R. J., Sauquet, E., Stagge, J. H. J. H., Wong, W. K. W. K., Scholz, P., Van Lanen, H. A. J. H. A. J., Adler, M. J. M.-J., Caillouet, L., Delus, C., Fendekova, M., Gailliez, S., Hannaford, J., Kingston, D., Van Loon, A. F. A. F., Mediero, L., Osuch, M., Romanowicz, R. J., Sauquet, E., Stagge, J. H. J. H. and Wong, W. K. W. K.: The European 2015 drought from a hydrological perspective, Hydrol. Earth Syst. Sci., 21(3), 3001–3024, doi:10.5194/hess-21-3001-2017, 2017.

Van Lanen, H. A. J. H. A. J., Laaha, G., Kingston, D. G. D. G., Gauster, T., Ionita, M., Vidal, J.-P. J. P., Vlnas, R., Tallaksen, L. M. L. M., Stahl, K., Hannaford, J., Delus, C., Fendekova, M., Mediero, L., Prudhomme, C., Rets, E., Romanowicz, R. J. R. J., Gailliez, S., Wong, W. K. W. K., Adler, M. J. M.-J., Blauhut, V., Caillouet, L., Chelcea, S., Frolova, N., Gudmundsson, L., Hanel, M., Haslinger, K., Kireeva, M., Osuch, M., Sauquet, E., Stagge, J. H. J. H. and Van Loon, A. F. A. F.: Hydrology needed to manage droughts: the 2015 European case, Hydrol. Process., 30(17), 3097–3104, doi:10.1002/hyp.10838, 2016.

622 Leonard, M., Westra, S., Phatak, A., Lambert, M., van den Hurk, B., McInnes, K., Risbey, J., Schuster, S., Jakob, D. and
623 Stafford-Smith, M.: A compound event framework for understanding extreme impacts, WIREs Clim. Chang., 5(1), 113–
624 128, doi:https://doi.org/10.1002/wcc.252, 2014.

625 Lorenz, R., Stalhandske, Z. and Fischer, E. M.: Detection of a Climate Change Signal in Extreme Heat, Heat Stress, and
626 Cold in Europe From Observations, Geophys. Res. Lett., 46(14), 8363–8374, doi:https://doi.org/10.1029/2019GL082062,
627 2019.

628 Malinovic-Milicevic, S., Radovanovic, M. M., Stanojevic, G. and Milovanovic, B.: Recent changes in Serbian climate
629 extreme indices from 1961 to 2010, Theor. Appl. Climatol., 124(3), 1089–1098, doi:10.1007/s00704-015-1491-1, 2016.

630 Mann, H. B.: Nonparametric Tests Against Trend, Econometrica, 13(3), 245–259, doi:10.2307/1907187, 1945.

631 Micu, D. M., Amihaesei, V. A., Milian, N. and Cheval, S.: Recent changes in temperature and precipitation indices in the
632 Southern Carpathians, Romania (1961–2018), Theor. Appl. Climatol., 144(1), 691–710, doi:10.1007/s00704-021-03560-w,
633 2021.

634 Nagavciuc, V., Ionita, M., Perşoiu, A., Popa, I., Loader, N. J. and McCarroll, D.: Stable oxygen isotopes in Romanian oak
635 tree rings record summer droughts and associated large-scale circulation patterns over Europe, Clim. Dyn., 52(11),
636 doi:10.1007/s00382-018-4530-7, 2019.

637 Najibi, N., Devineni, N., Lu, M. and Perdigão, R. A. P.: Coupled flow accumulation and atmospheric blocking govern flood
638 duration, npj Clim. Atmos. Sci., 2(1), 19, doi:10.1038/s41612-019-0076-6, 2019.

639 Perkins, S. E. and Alexander, L. V: On the Measurement of Heat Waves, J. Clim., 26(13), 4500–4517, doi:10.1175/JCLI-D-
640 12-00383.1, 2013.

641 Porebska, M. and Zdunek, M.: Analysis of extreme temperature events in Central Europe related to high pressure blocking
642 situations in 2001?2011, Meteorol. Zeitschrift, 22(5), 533–540, doi:10.1127/0941-2948/2013/0455, 2013.

643 Prăvălie, R., Bandoc, G., Patriche, C. and Tomescu, M.: Spatio-temporal trends of mean air temperature during 1961–2009
644 and impacts on crop (maize) yields in the most important agricultural region of Romania, Stoch. Environ. Res. Risk Assess.,
645 31(8), 1923–1939, doi:10.1007/s00477-016-1278-7, 2017.

646 Raymond, C., Horton, R. M., Zscheischler, J., Martius, O., AghaKouchak, A., Balch, J., Bowen, S. G., Camargo, S. J., Hess,
647 J., Kornhuber, K., Oppenheimer, M., Ruane, A. C., Wahl, T. and White, K.: Understanding and managing connected
648 extreme events, Nat. Clim. Chang., 10(7), 611–621, doi:10.1038/s41558-020-0790-4, 2020.

649 Rey, G., Jougla, E., Fouillet, A., Pavillon, G., Bessemoulin, P., Frayssinet, P., Clavel, J. and Hémon, D.: The impact of
650 major heat waves on all-cause and cause-specific mortality in France from 1971 to 2003, Int. Arch. Occup. Environ. Health,
651 80(7), 615–626, doi:10.1007/s00420-007-0173-4, 2007.

652 Ridder, N. N., Pitman, A. J., Westra, S., Ukkola, A., Do, H. X., Bador, M., Hirsch, A. L., Evans, J. P., Di Luca, A. and
653 Zscheischler, J.: Global hotspots for the occurrence of compound events, Nat. Commun., 11(1), 5956, doi:10.1038/s41467-
654 020-19639-3, 2020.

655 Rimbu, N., Dima, M., Lohmann, G. and Stefan, S.: Impacts of the North Atlantic Oscillation and the El Niño-Southern
656 Oscillation on Danube river flow variability, Geophys. Res. Lett., 31(23), 1–4, doi:10.1029/2004GL020559, 2004.

657 Rimbu, N., Lohmann, G. and Ionita, M.: Interannual to multidecadal Euro-Atlantic blocking variability during winter and its
658 relationship with extreme low temperatures in Europe, J. Geophys. Res. Atmos., 119(24), 13621–13636,
659 doi:10.1002/2014JD021983, 2014.

660 Robinson, P. J.: On the Definition of a Heat Wave, J. Appl. Meteorol., 40(4), 762–775, doi:10.1175/1520-
661 0450(2001)040<0762:OTDOAH>2.0.CO;2, 2001.

Russo, A., Gouveia, C. M., Dutra, E., Soares, P. M. M. and Trigo, R. M.: The synergy between drought and extremely hot summers in the Mediterranean, Environ. Res. Lett., 14(1), 014011, doi:10.1088/1748-9326/aaf09e, 2019.

Rusticucci, M., Barrucand, M. and Collazo, S.: Temperature extremes in the Argentina central region and their monthly relationship with the mean circulation and ENSO phases, Int. J. Climatol., 37(6), 3003–3017, doi:https://doi.org/10.1002/joc.4895, 2017.

Scherrer, S. C., Croci-Maspoli, M., Schwierz, C. and Appenzeller, C.: Two-dimensional indices of atmospheric blocking and their statistical relationship with winter climate patterns in the Euro-Atlantic region, Int. J. Climatol., 26(2), 233–249, doi:10.1002/joc.1250, 2006.

Schubert, S. D., Wang, H., Koster, R. D., Suarez, M. J. and Groisman, P. Y.: Northern Eurasian heat waves and droughts, J. Clim., 27(9), 3169–3207, doi:10.1175/JCLI-D-13-00360.1, 2014.

Schubert, S. D., Stewart, R. E., Wang, H., Barlow, M., Berbery, E. H., Cai, W., Hoerling, M. P., Kanikicharla, K. K., Koster, R. D., Lyon, B., Mariotti, A., Mechoso, C. R., Müller, O. V., Rodriguez-Fonseca, B., Seager, R., Senevirante, S. I., Zhang, L. and Zhou, T.: Global meteorological drought: A synthesis of current understanding with a focus on sst drivers of precipitation deficits, J. Clim., doi:10.1175/JCLI-D-15-0452.1, 2016.

Sen, P. K.: Estimates of the Regression Coefficient Based on Kendall's Tau, J. Am. Stat. Assoc., 63(324), 1379–1389, doi:10.1080/01621459.1968.10480934, 1968.

Seneviratne, S. I., Nicholls, N., Easterling, D., Goodess, C. M., Kanae, S., Kossin, J., Luo, Y., Marengo, J., McInnes, K., Rahimi, M., Reichstein, M., Sorteberg, A., Vera, C., Zhang, X., Rusticucci, M., Semenov, V., Alexander, L. V, Allen, S., Benito, G., Cavazos, T., Clague, J., Conway, D., Della-Marta, P. M., Gerber, M., Gong, S., Goswami, B. N., Hemer, M., Huggel, C., van den Hurk, B., Kharin, V. V, Kitoh, A., Tank, A. M. G. K., Li, G., Mason, S., McGuire, W., van Oldenborgh, G. J., Orlowsky, B., Smith, S., Thiaw, W., Velegrakis, A., Yiou, P., Zhang, T., Zhou, T. and Zwiers, F. W.: Changes in Climate Extremes and their Impacts on the Natural Physical Environment, in Managing the Risks of Extreme Events and Disasters to Advance Climate Change Adaptation: Special Report of the Intergovernmental Panel on Climate Change, edited by C. B. Field, Q. Dahe, T. F. Stocker, and V. Barros, pp. 109–230, Cambridge University Press, Cambridge., 2012.

Sfîcă, L., Croitoru, A.-E., Iordache, I. and Ciupertea, A.-F.: Synoptic Conditions Generating Heat Waves and Warm Spells in Romania, Atmosphere (Basel)., 8(3), doi:10.3390/atmos8030050, 2017.

Shevchenko, O., Lee, H., Snizhko, S. and Mayer, H.: Long-term analysis of heat waves in Ukraine, Int. J. Climatol., 34(5), 1642–1650, doi:https://doi.org/10.1002/joc.3792, 2014.

Smoyer-Tomic, K. E., Kuhn, R. and Hudson, A.: Heat Wave Hazards: An Overview of Heat Wave Impacts in Canada, Nat. Hazards, 28(2), 465–486, doi:10.1023/A:1022946528157, 2003.

Spinoni, J., Naumann, G., Vogt, J. V. and Barbosa, P.: The biggest drought events in Europe from 1950 to 2012, J. Hydrol. Reg. Stud., 3, 509–524, doi:10.1016/j.ejrh.2015.01.001, 2015.

Stegehuis, A. I., Vogel, M. M., Vautard, R., Ciais, P., Teuling, A. J. and Seneviratne, S. I.: Early Summer Soil Moisture Contribution to Western European Summer Warming, J. Geophys. Res. Atmos., 126(17), e2021JD034646, doi:https://doi.org/10.1029/2021JD034646, 2021.

Swain, D. L., Horton, D. E., Singh, D. and Diffenbaugh, N. S.: Trends in atmospheric patterns conducive to seasonal precipitation and temperature extremes in California, Sci. Adv., 2(4), 1–14, doi:10.1126/sciadv.1501344, 2016.

Tibaldi, S. and Molteni, F.: On the operational predictability of blocking, Tellus, 42(A), 343–365, 1990.

Tomczyk, A. M. and Bednorz, E.: Heat waves in Central Europe and their circulation conditions, Int. J. Climatol., 36(2), 770–782, doi:https://doi.org/10.1002/joc.4381, 2016.

703 Tomczyk, A. M., Półrolniczak, M. and Bednorz, E.: Circulation Conditions' Effect on the Occurrence of Heat Waves in
704 Western and Southwestern Europe, Atmosphere (Basel)., 8(2), doi:10.3390/atmos8020031, 2017.

705 Tomozeiu, R., Stefan, S. and Busuioc, A.: Winter precipitation variability and large-scale circulation patterns in Romania,
706 Theor. Appl. Clim., 81, 193–201, doi:10.1007/s00704-004-0082-3, 2005.

707 Twardosz, R. and Kossowska-Cezak, U.: Exceptionally hot summers in Central and Eastern Europe (1951-2010), Theor.
708 Appl. Climatol., 112(3–4), 617–628, doi:10.1007/s00704-012-0757-0, 2013.

709 Vaideanu, P., Dima, M., Pirloaga, R. and Ionita, M.: Disentangling and quantifying contributions of distinct forcing factors
710 to the observed global sea level pressure field, Clim. Dyn., 54(3–4), doi:10.1007/s00382-019-05067-7, 2020.

711 Vicente-Serrano, S. M. and López-Moreno, J. I.: Nonstationary influence of the North Atlantic Oscillation on European
712 precipitation, J. Geophys. Res. Atmos., 113(20), 1–14, doi:10.1029/2008JD010382, 2008.

713 Vicente-Serrano, S. M., Beguería, S. and López-Moreno, J. I.: A multiscalar drought index sensitive to global warming: The
714 standardized precipitation evapotranspiration index, J. Clim., 23(7), 1696–1718, doi:10.1175/2009JCLI2909.1, 2010.

715 Zscheischler, J. and Seneviratne, S. I.: Dependence of drivers affects risks associated with compound events, Sci. Adv.,
716 3(6), 1–11, doi:10.1126/sciadv.1700263, 2017.

717 Zscheischler, J., Westra, S., Van Den Hurk, B. J. J. M., Seneviratne, S. I., Ward, P. J., Pitman, A., Aghakouchak, A.,
718 Bresch, D. N., Leonard, M., Wahl, T. and Zhang, X.: Future climate risk from compound events, Nat. Clim. Chang., 8(6),
719 469–477, doi:10.1038/s41558-018-0156-3, 2018.

720

721

722

723

724

725

726

727

728

729

730

731

732

733

734

735

736 ***Author Contributions***. VN, PS and MI designed the study, wrote the paper and interpret the results. All authors (i.e. VN, PS
737 and MI) contributed equally to the article**.**

738 ***Acknowledgments***. Viorica Nagavciuc was supported by a grant of the Ministry of Research, Innovation and Digitization,
739 CNCS/CCCDI – UEFISCDI, project number PN-III-P1-1.1-PD-2019-0469, within PNCDI III. Monica Ionita and Patrick
740 Scholz are supported by Helmholtz Association through the joint program "Changing Earth - Sustaining our Future" (PoF IV)
741 program of the AWI. Funding by the Helmholtz Climate Initiative REKLIM, the AWI Strategy Fund Project - PalEX and the
742 project S2: Improved parameterisations and numerics in climate models, of the collaborative Research Center TRR181
743 "Energy Trasnfer in the Atmosphere and Ocean" (DFG) - Projektnummer 274762653 are gratefully acknowledged.

744 ***Data availability***. The data that support the findings of this study are available from the corresponding author upon reasonable
745 request.

746 ***Financial support***. The article processing charges for this open access publication were covered by the Alfred Wegener
747 Institute, Helmholtz Centre for Polar and Marine Research (AWI).

748 ***Competing interests***. The authors declare that they have no conflict of interest.

749

750

751

752

753

754

755

756

757

758

759

760

761

762

763

764

765

766

767

Figure 1. The topographic map of Romania and the location of the country at European level

768

769

770
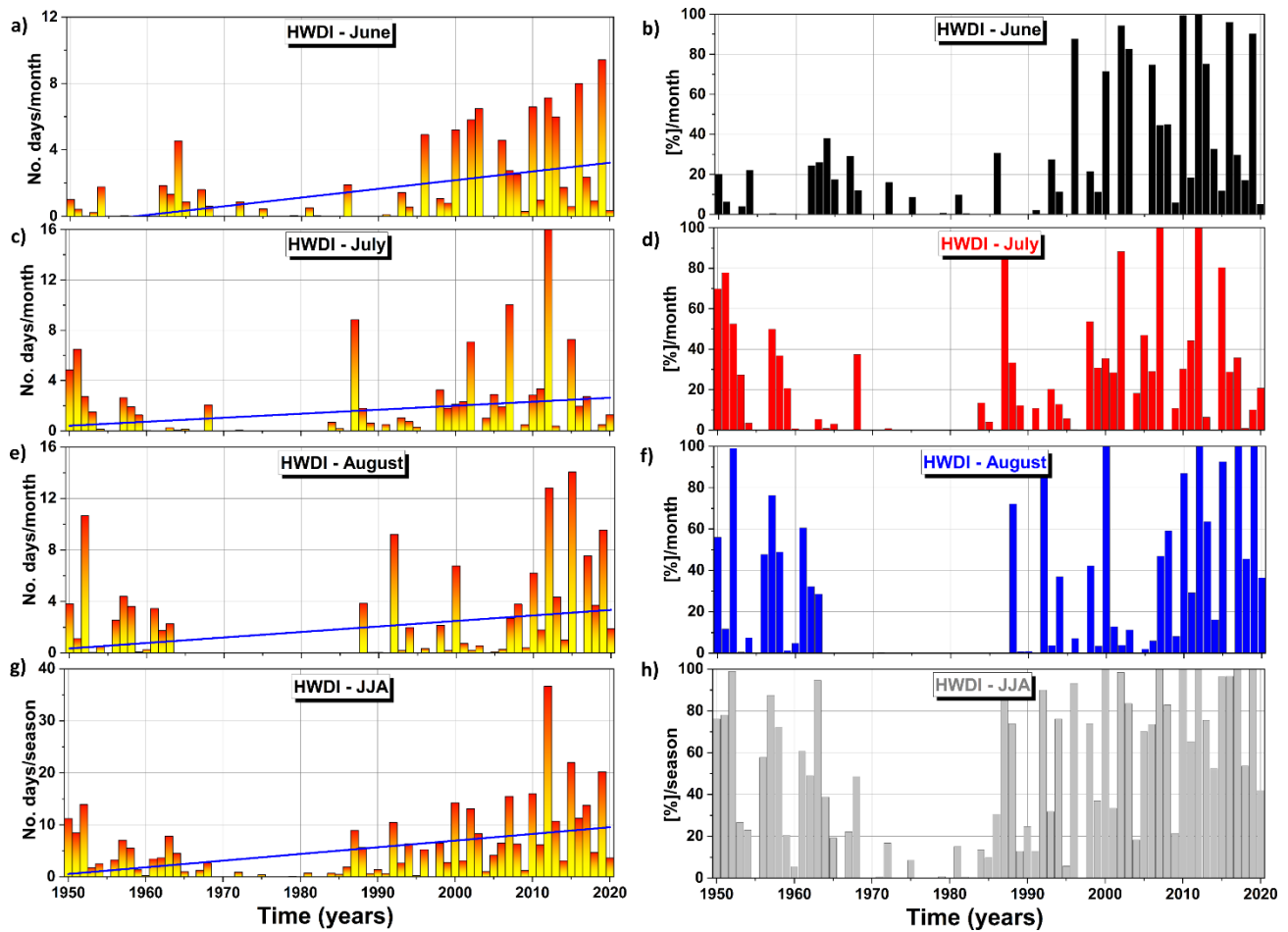
Figure 2. Monthly and seasonal temporal evolution of the summer heat waves duration (HWDI) averaged at country level (left column) and the temporal evolution of the percentage area (AREA) affected by heat waves (right column) over period 1950 – 2020: a) June HWDI; b) June AREA; c) July HWDI; d) July AREA; e) August HWDI; f) August AREA; g) Summer (JJA) HWDI and h) Summer (JJA) AREA. The blue line indicates the linear trend.

771

772

773
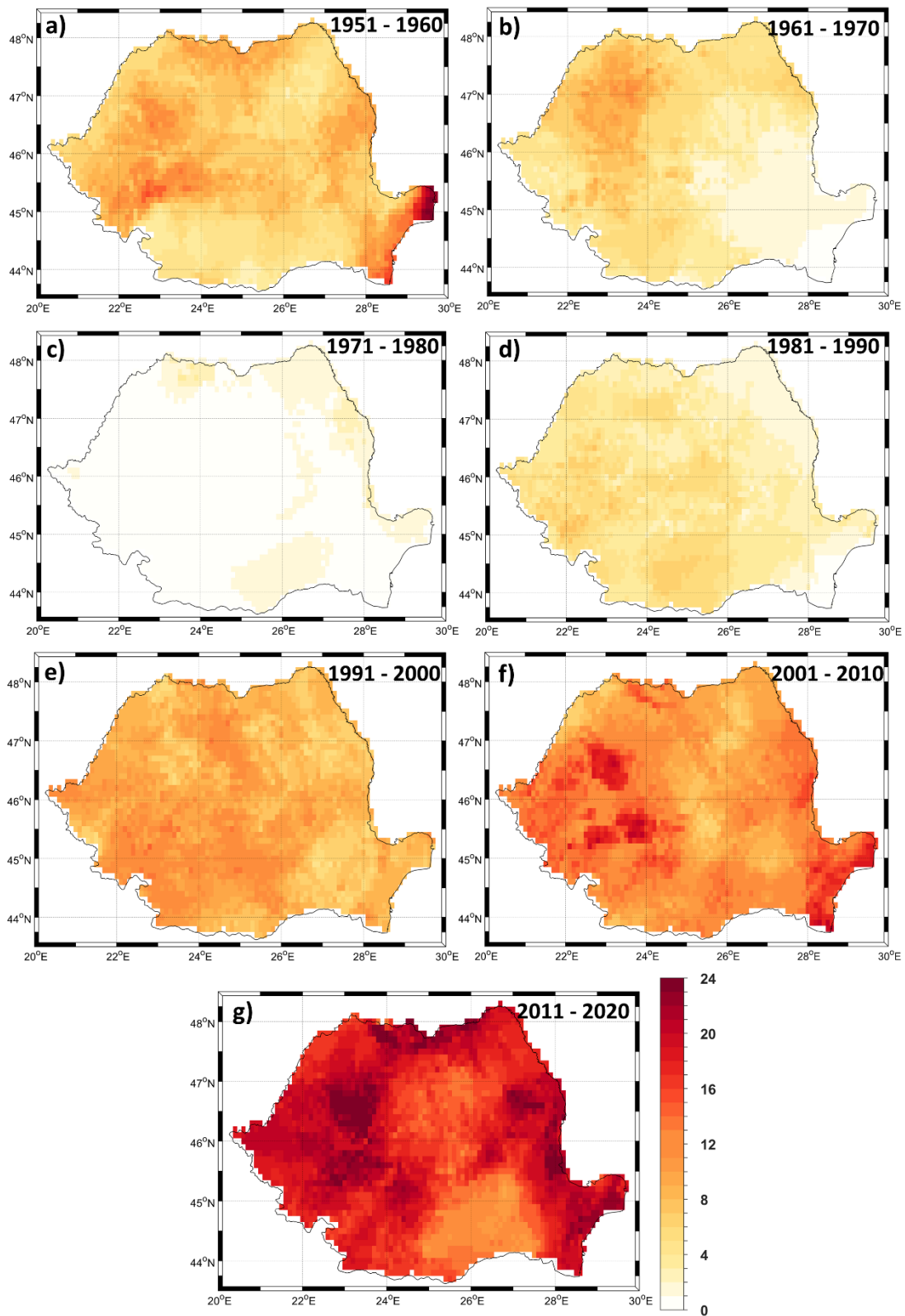
Figure 3. Decadal frequency of the number of summer heat waves (HWs) per decade over the last 70 years: a) 1951 – 1960; b) 1961 – 1970; c) 1971 – 1980; d) 1981 – 1990; e) 1991 – 2000; f) 2001 – 2010 and g) 2011 – 2020. Units: number of HWs/decade.
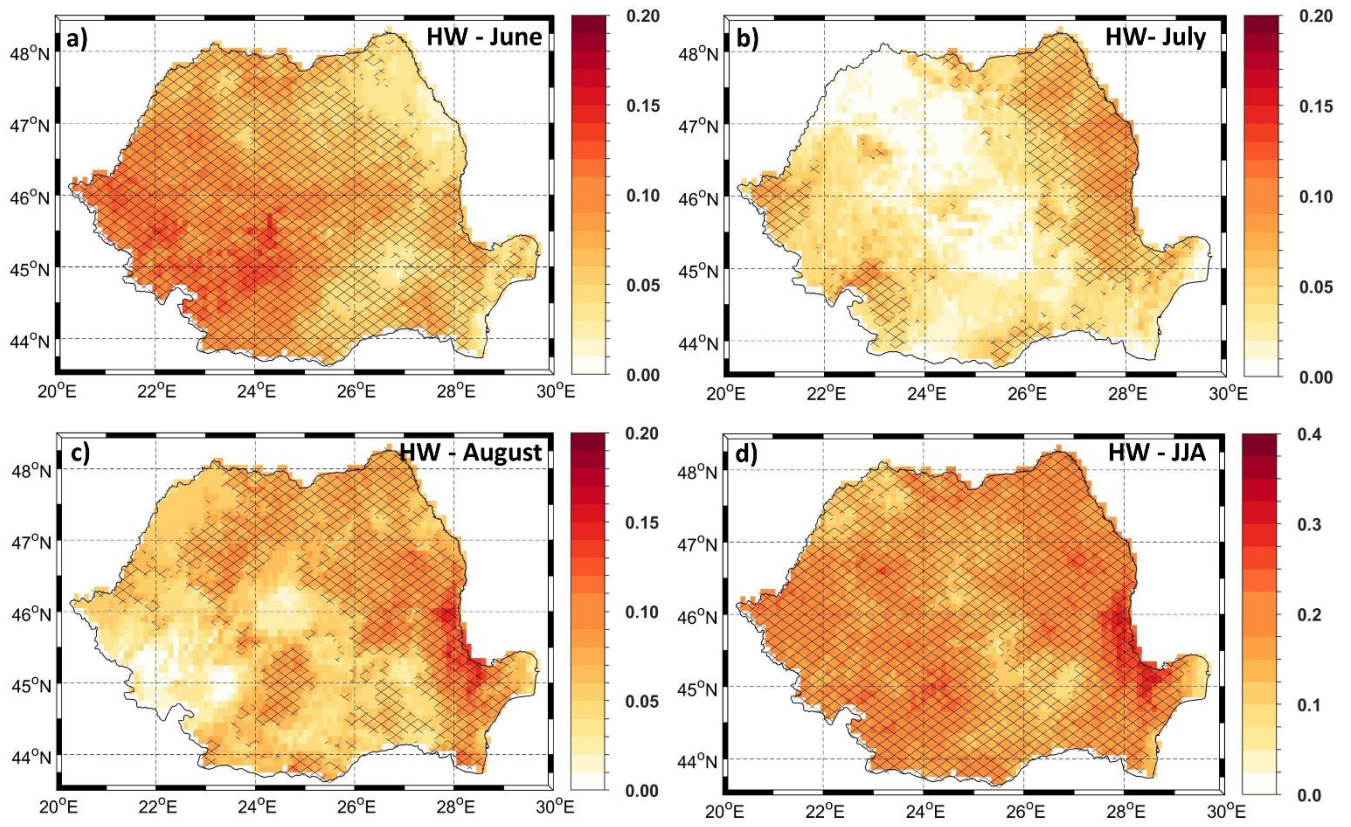
Figure 4. Linear trend of the number heat waves for: a) June; b) July; c) August and d) JJA. Stipples indicate statistically significant trends. Units: number of HWs/decade. Analyzed period 1950 – 2020.

774

775

776

777

778

779

780

781

782
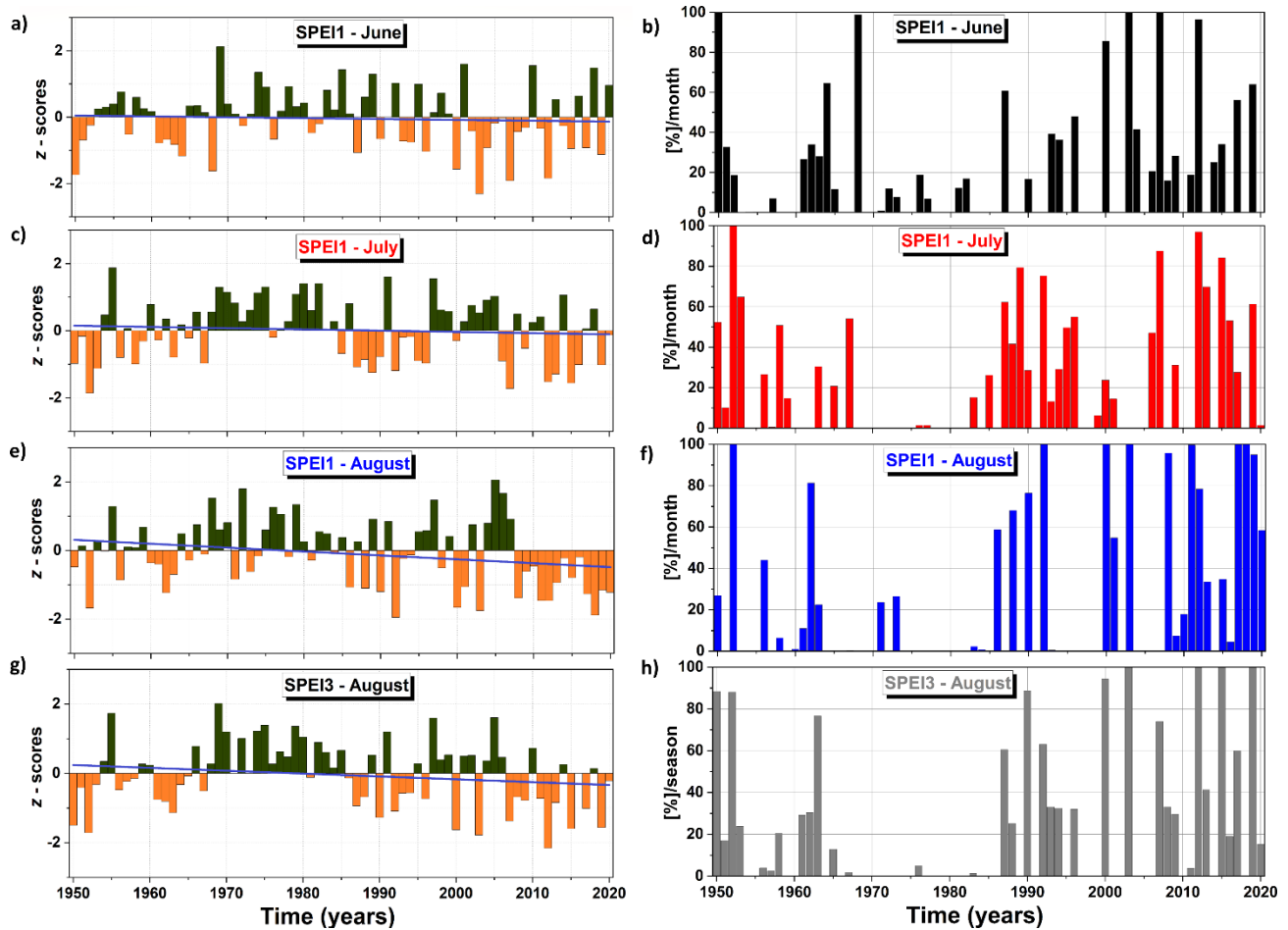
Figure 5. Monthly and seasonal temporal evolution of the SPEI index averaged at country level (left column) and the temporal evolution of the percentage area (AREA) affected by drought conditions (SPEI ≤ -1) right column) over period 1950 – 2020: a) June SPEI1; b) June drought AREA; c) July SPEI1; d) July drought AREA; e) August SPEI1; f) August drought AREA; g) August SPEI3 (indicator of dry/wet condition over the summer seasons) and h) August SPEI3 drought AREA. The blue line indicates the linear trend line.

783

784
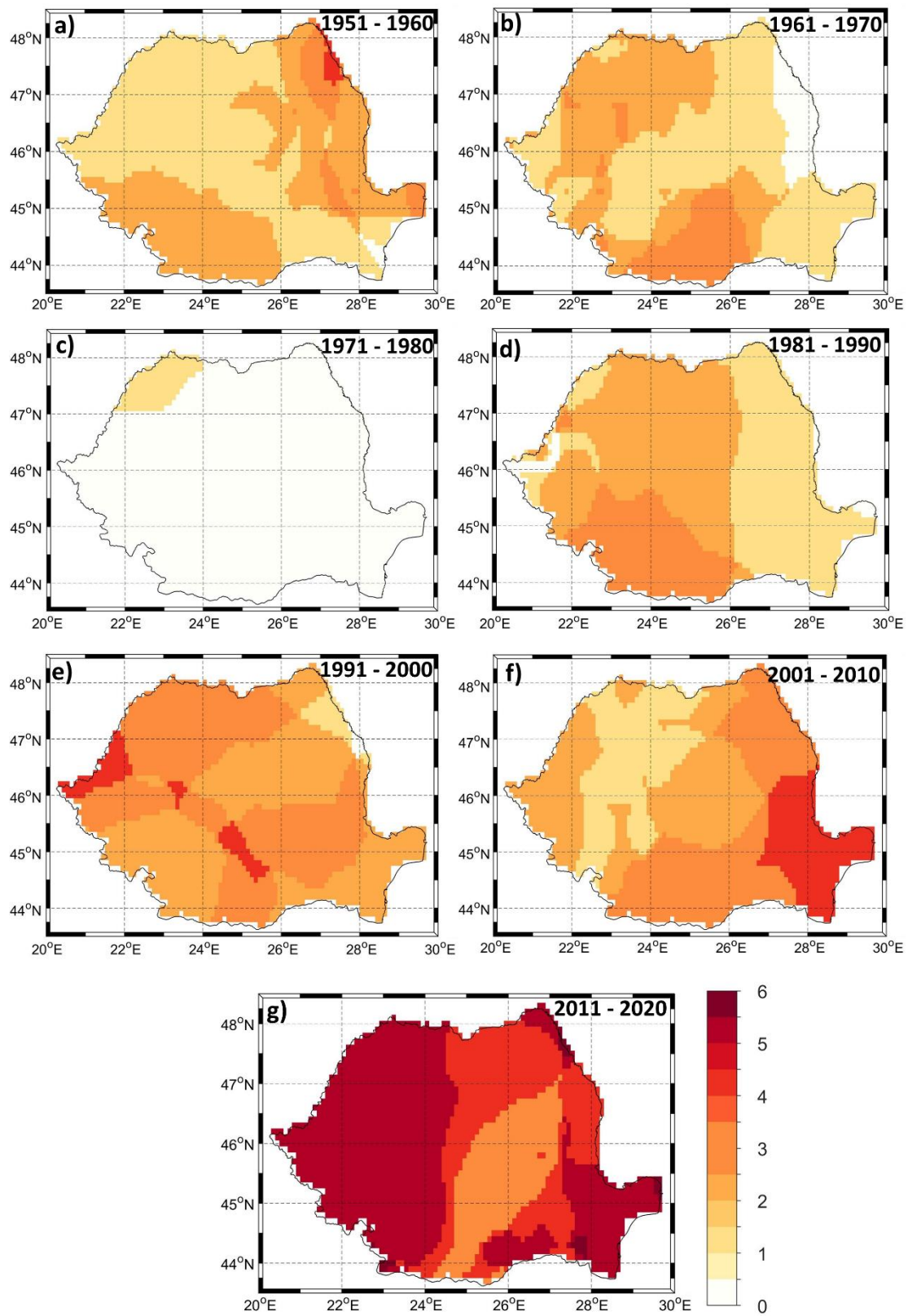
Figure 6. Decadal frequency of August SPEI3 over the last 70 years for the cases when August SPEI3 ≤ -1: a) 1951 – 1960; b) 1961 – 1970; c) 1971 – 1980; d) 1981 – 1990; e) 1991 – 2000; f) 2001 – 2010 and g) 2011 – 2020. Units: number of dry summers/decade.
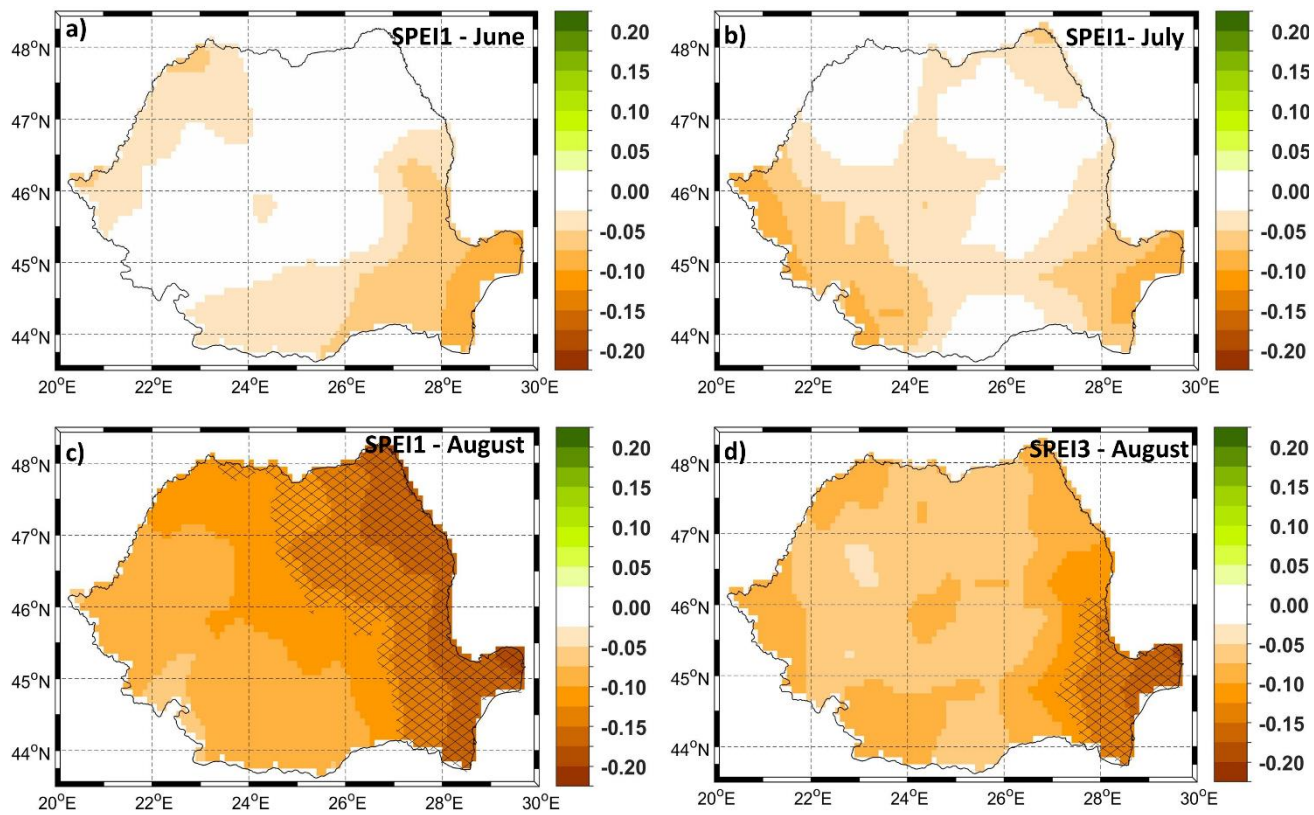
Figure 7. Linear trend of: a) June SPEI1; b) July SPEI1; c) August SPEI1 and d) the Augsut SPEI3. Stipples indicate statistically significant trends. Units: number of z-scores/decade. Analyzed period 1950 – 2020.

785

786

787

788

789

790

791

792

793

794

795

796

797
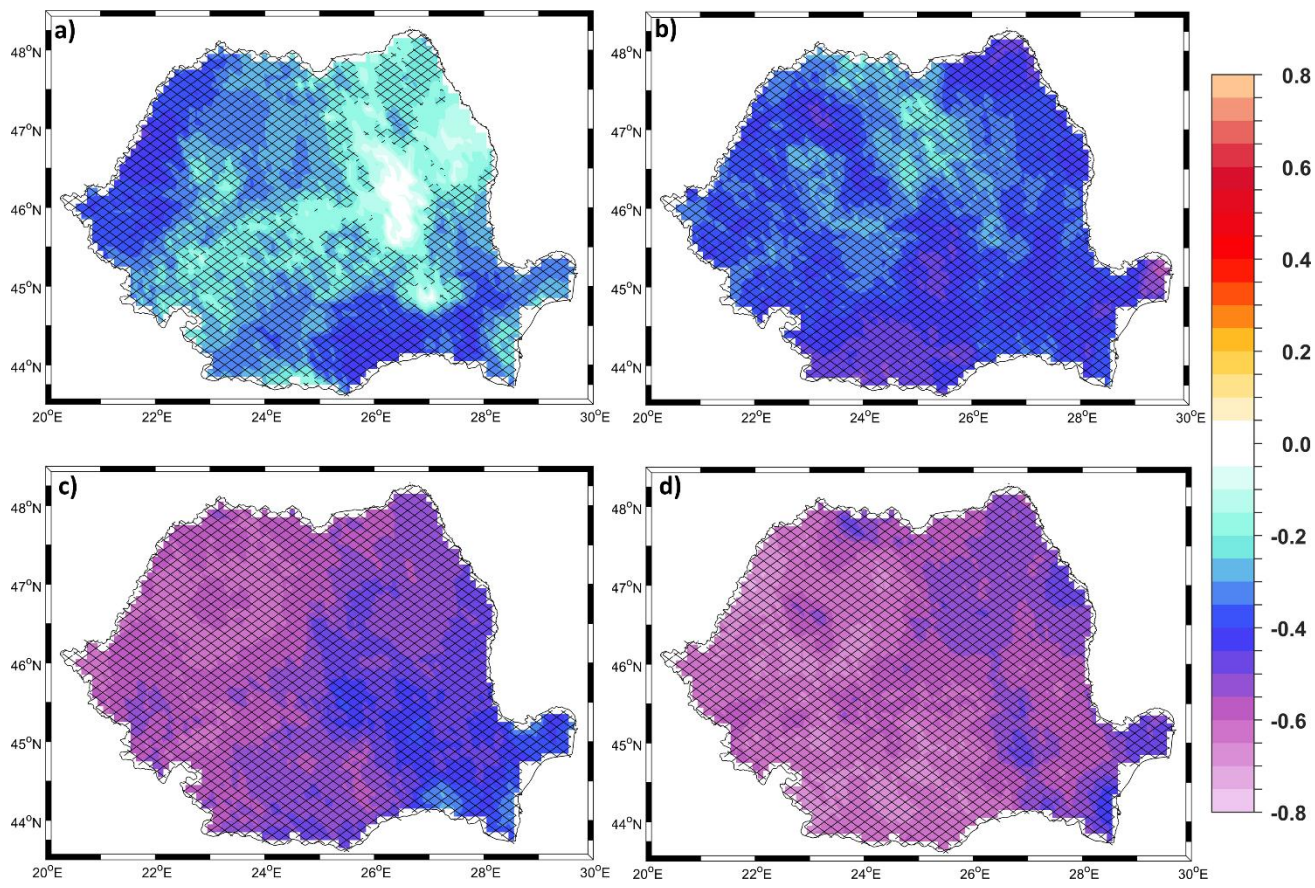
Figure 8. Spatial correlation between: a) June SPEI1 and June HWDI; b) July SPEI1 and July HWDI; c) August SPEI3 and HDWI August and d) August SPEI3 and JJA HWDI. The regions where the correlations are statistically significant (95% significance level) are hatched.

798

799

800

801

802

803

804

805
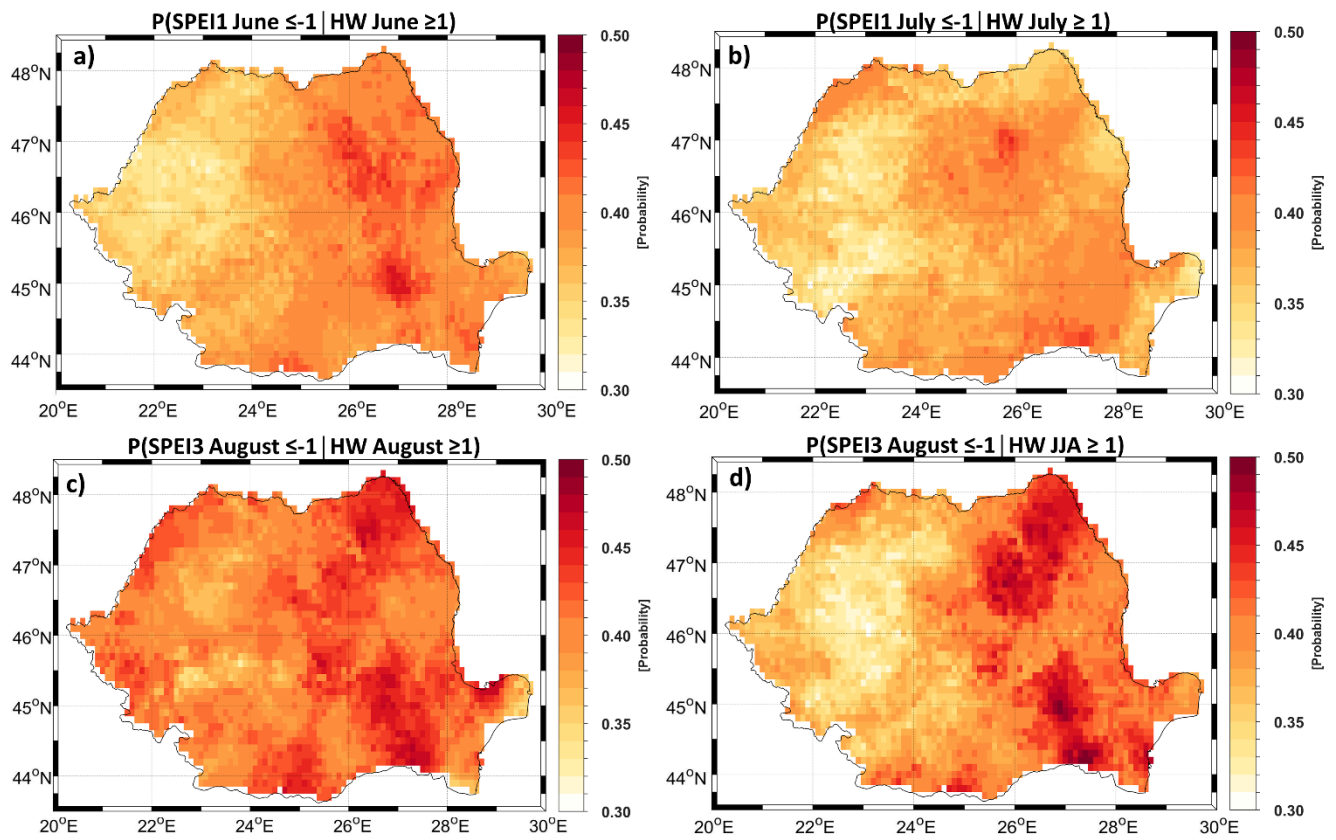
Figure 9. Conditional probability of occurrence of hot (HW ≥ 1) and dry (SPEI ≤ -1) events: a) June SPEI1 and June HW; b) July SPEI 1 and July HW; c) August SPEI3 and August HW and; d) August SPEI3 and JJA HW 1981 – 1990.
.
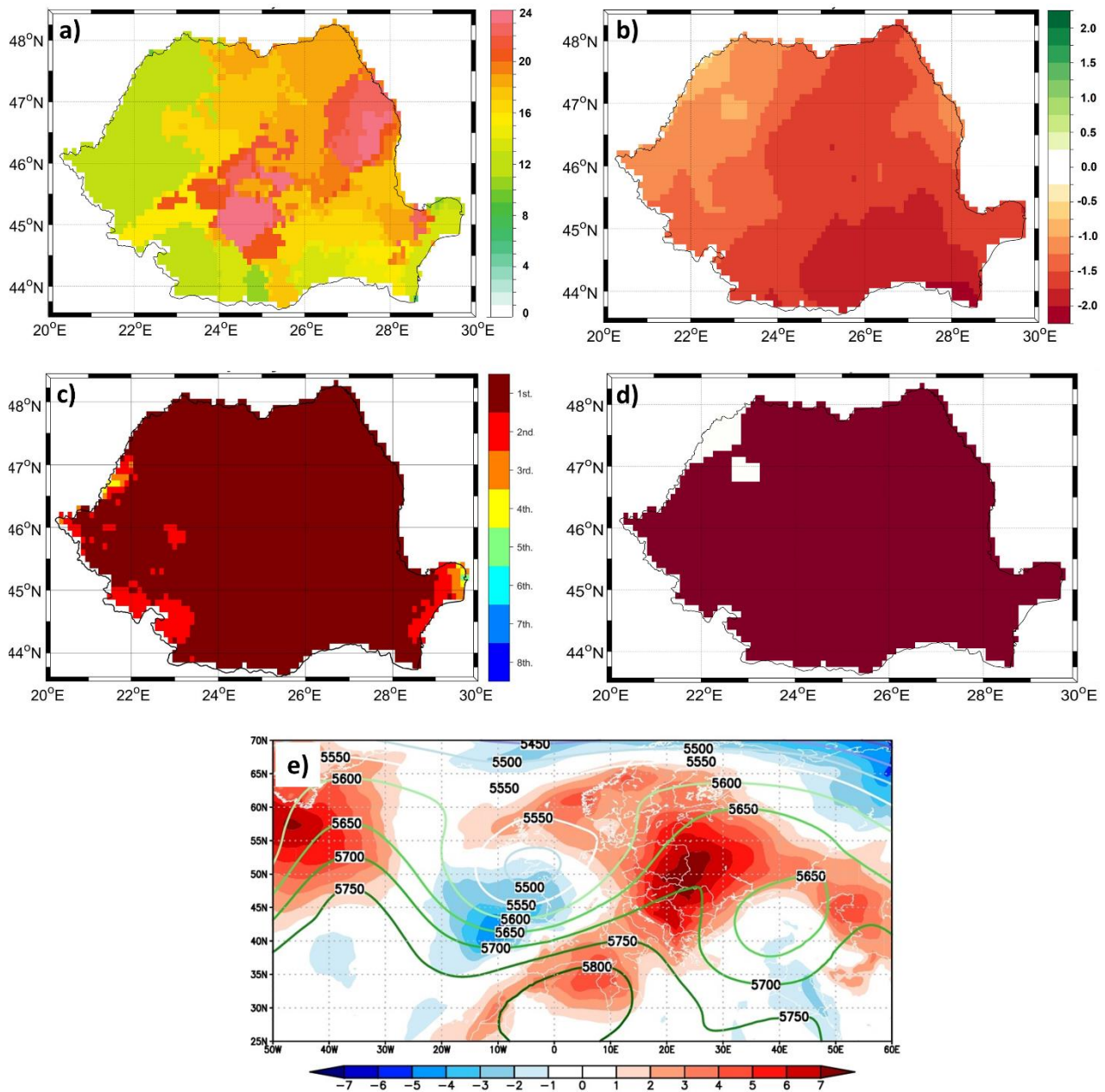
Figure 10. a) HWDI for July 2012; b) SPEI1 for July 2012; c) Top-eight ranking of TX90p for July 2012 (1st means the, hottest (Tx90p) since 1950, 2nd signifies the second hottest, etc., and all ranks >8 are shown in white); d) CHD for June 2012 (the dark red color indicates the grid points affected by a CHD) and e) daily Z500 (contour lines) and TT850 anomalies (shaded colors) averaged over the period 25 - 30.07.2012.
Units: a) days/month; e) Z500 (m) and TT850 (°C). For c) the analyzed period is 1950–2020.

806

807

808
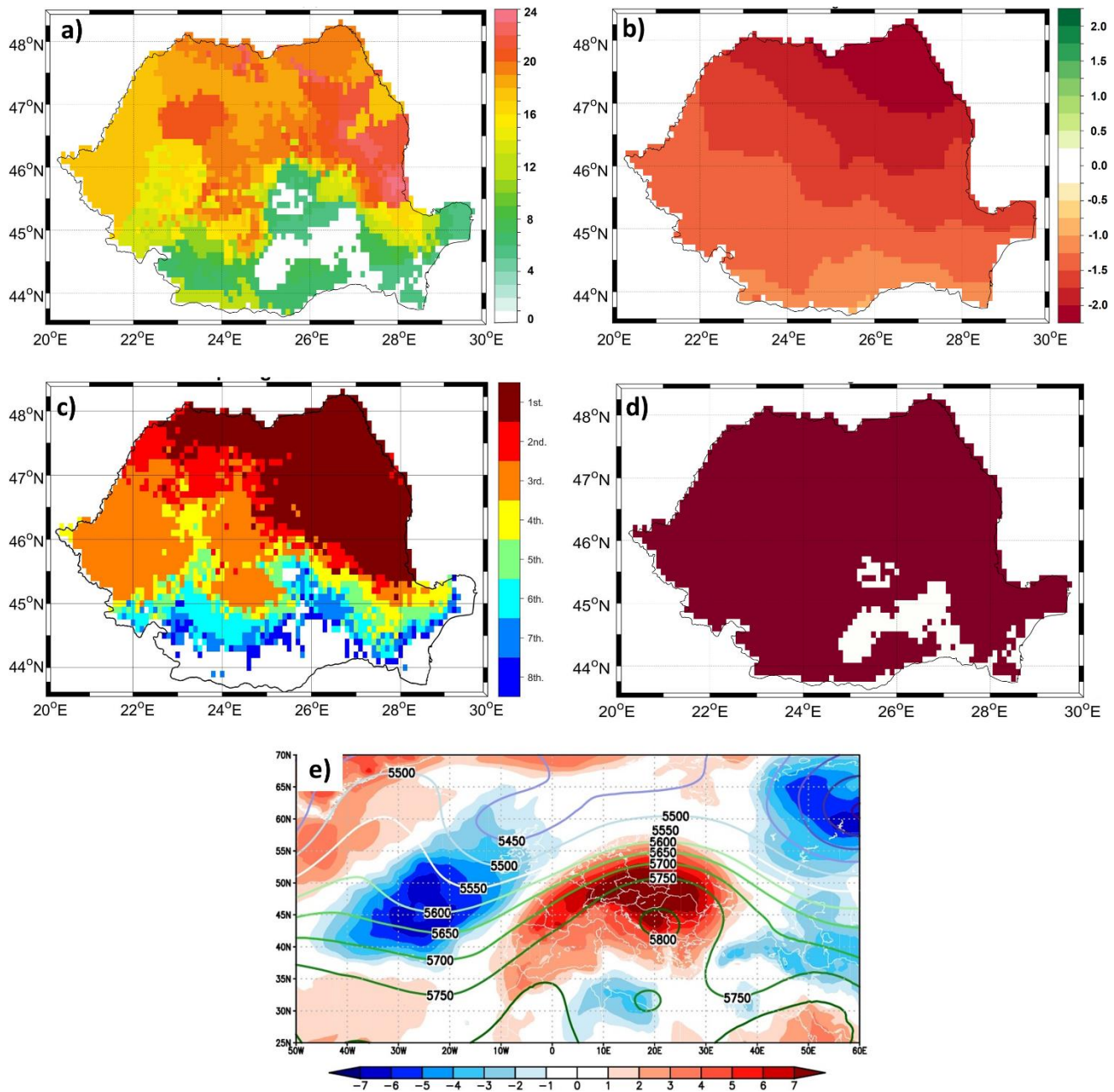
Figure 11. a) HWDI for August 2015; b) SPEI3 for August 2015; c) Top-eight ranking of TX90p for August 2015 (1st means the, hottest (Tx90p) since 1950, 2nd signifies the second hottest, etc., and all ranks >8 are shown in white); d) CHD for August 2015 (the dark red color indicates the grid points affected by a CHD) and e) daily Z500 (contour lines) and TT850 anomalies (shaded colors) averaged over the period 28 - 31.08.2015. Units: a) days/month; e) Z500 (m) and TT850 (°C). For c) the analyzed period is 1950–2020.

809

810

811
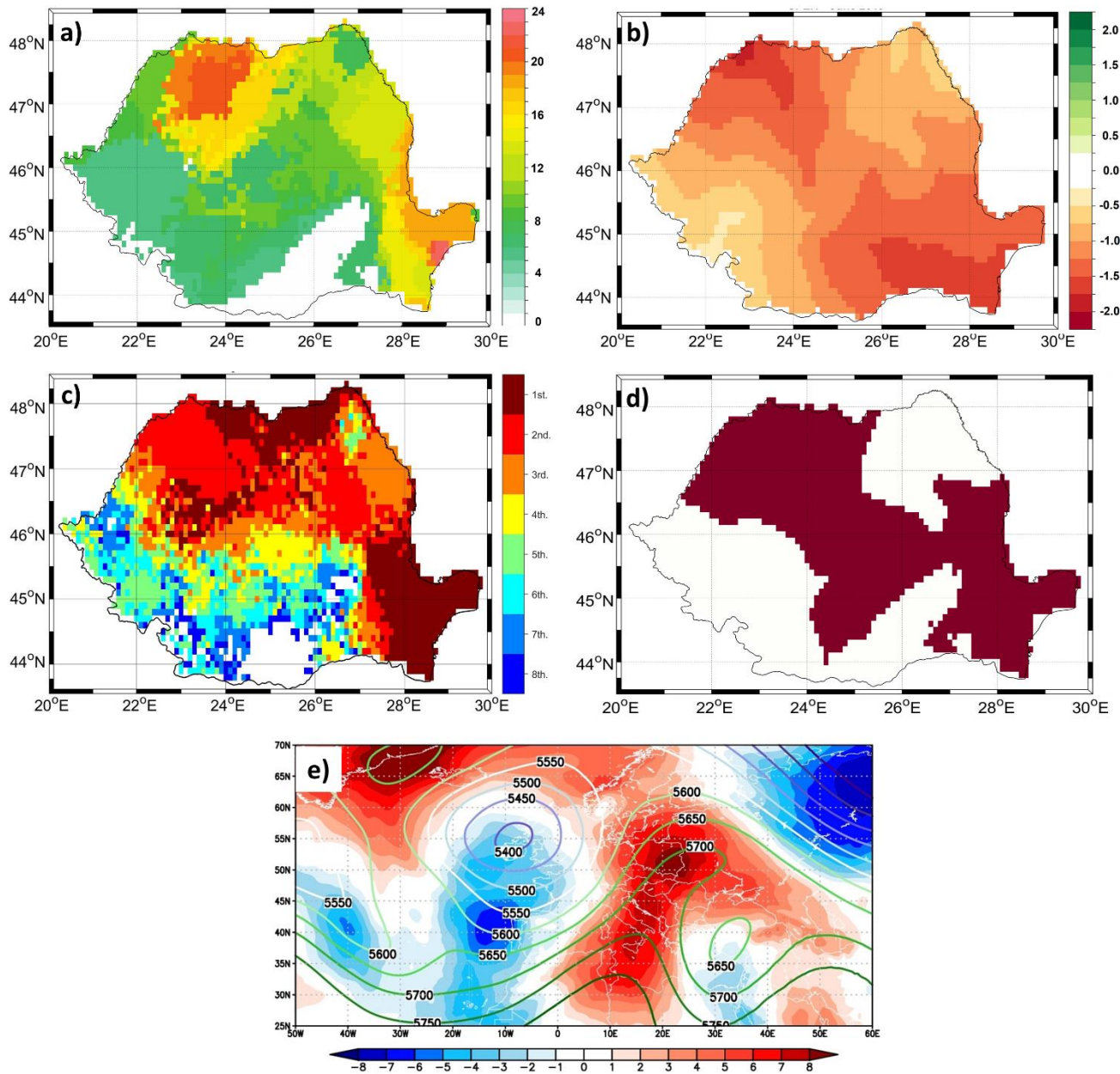
Figure 12. a) HWDI for June 2019; b) SPEI1 for June 2019; c) Top-eight ranking of TX90p for June 2019 (1st means the, hottest (Tx90p) since 1950, 2nd signifies the second hottest, etc., and all ranks >8 are shown in white); d) CHD for June 2019 (the dark red color indicates the grid points affected by a CHD) and e) daily Z500 (contour lines) and TT850 anomalies (shaded colors) averaged over the period 10 - 14.06.2019.
Units: a) days/month; e) Z500 (m) and TT850 (°C). For c) the analyzed period is 1950–2020.

812

813

814
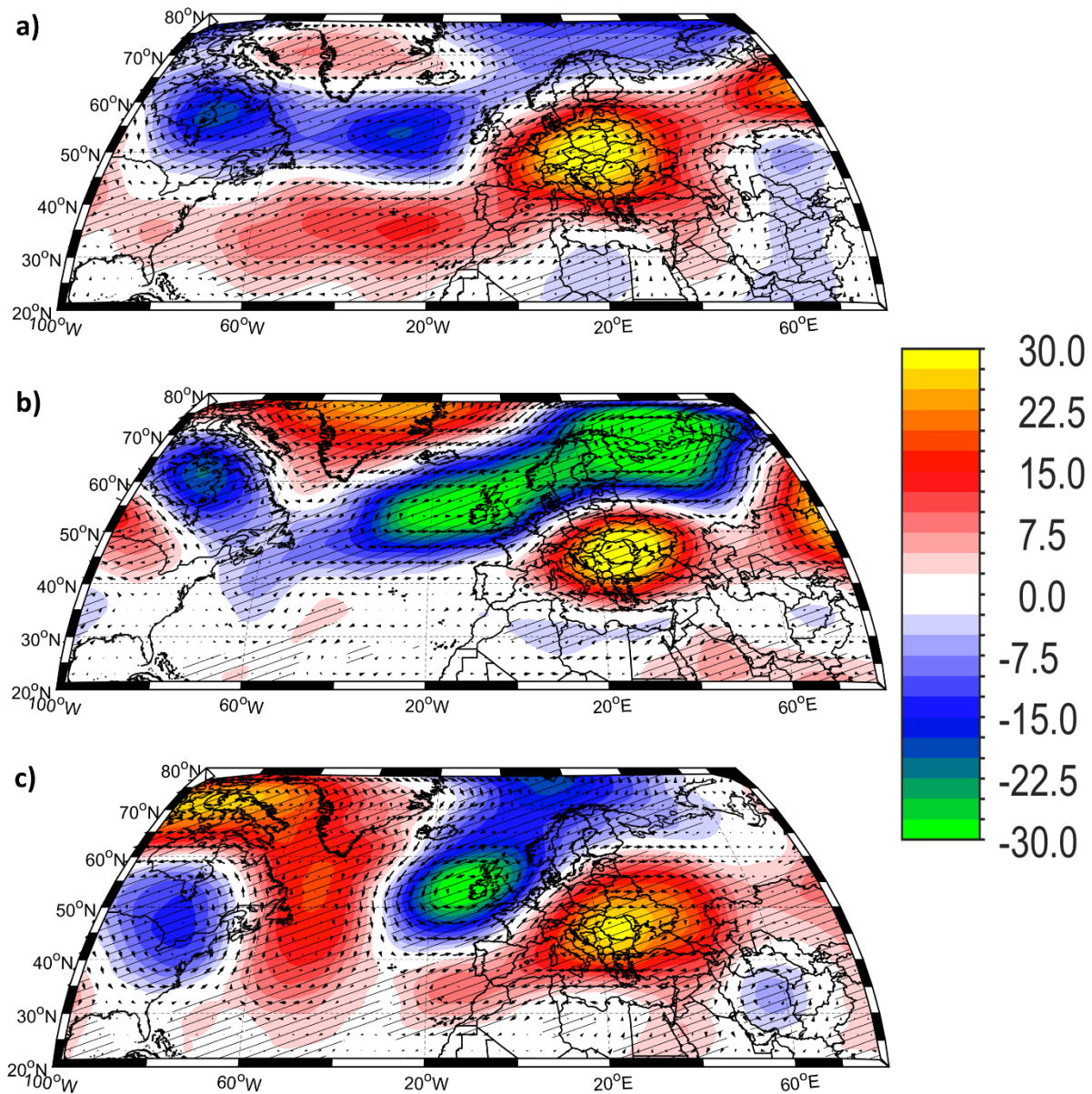
Figure 13. Large-scale atmospheric circulation patterns associated with the occurrence of monthly heat waves in Romania: a) The high composite map of June geopotential height at 500 mb (Z500) and the wind vectors at 500 mb corresponding to the cases when the area cover by a heat waves was higher than 20% of the country (June HW AREA> 20%); b) as in a) but for July and c) as in a) but for August. The hatched areas indicate anomalies significant at 95% significance level based on a two-tailed t-test. Units: Z500 [m].

815

816

817

818
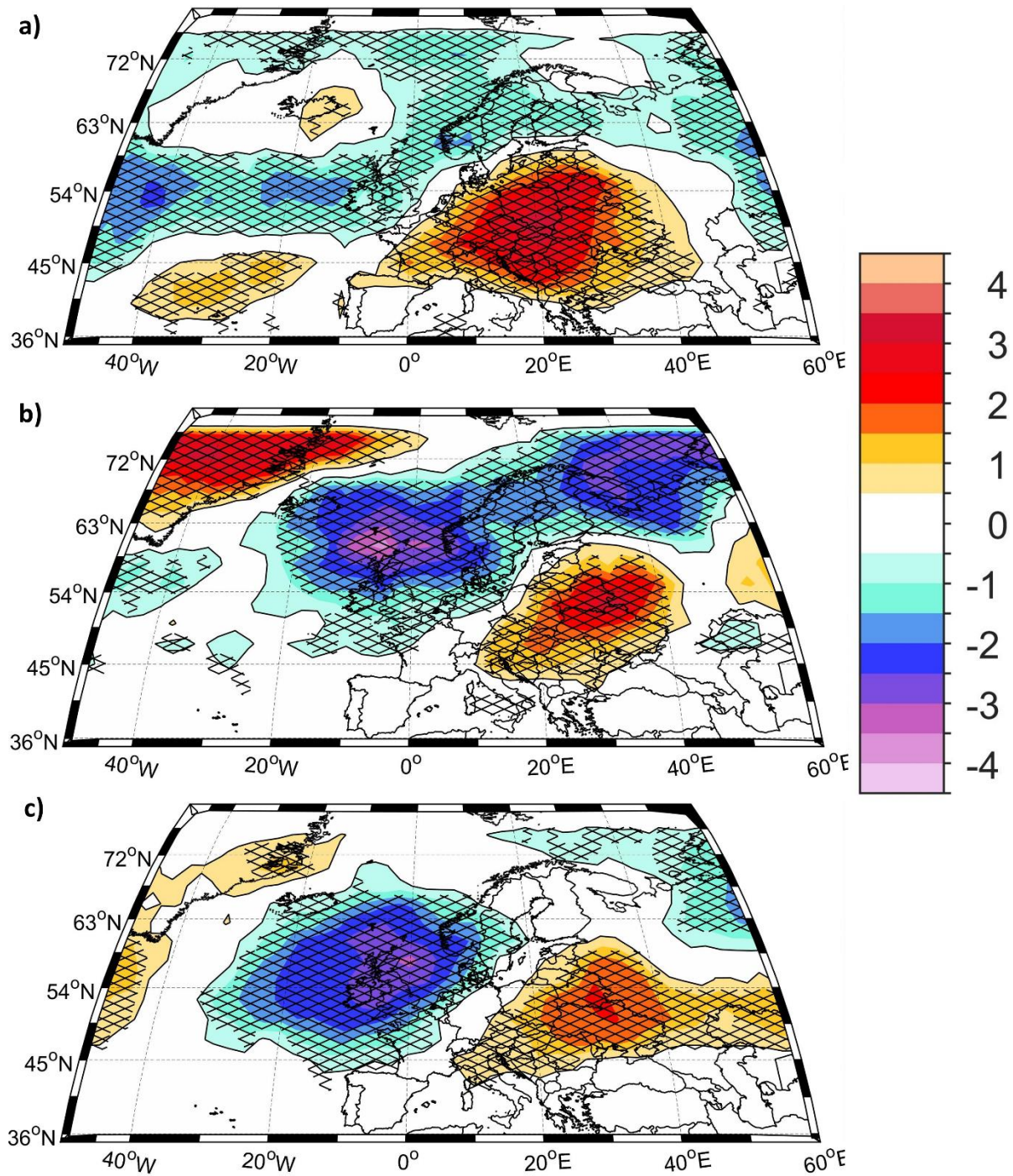
Figure 14. Frequency of the 2D atmospheric blocking associated with the occurrence of monthly heat waves in the central part of Europe: a) The high composite map of June 2D atmospheric blocking corresponding to the cases when the area cover by a heat waves was higher than 20% of the country (June HW AREA> 20%); b) as in a) but for July and c) as in a) but for August. The hatched areas indicate anomalies significant at 95% significance level based on a two-tailed t-test. Units: days/month.

819
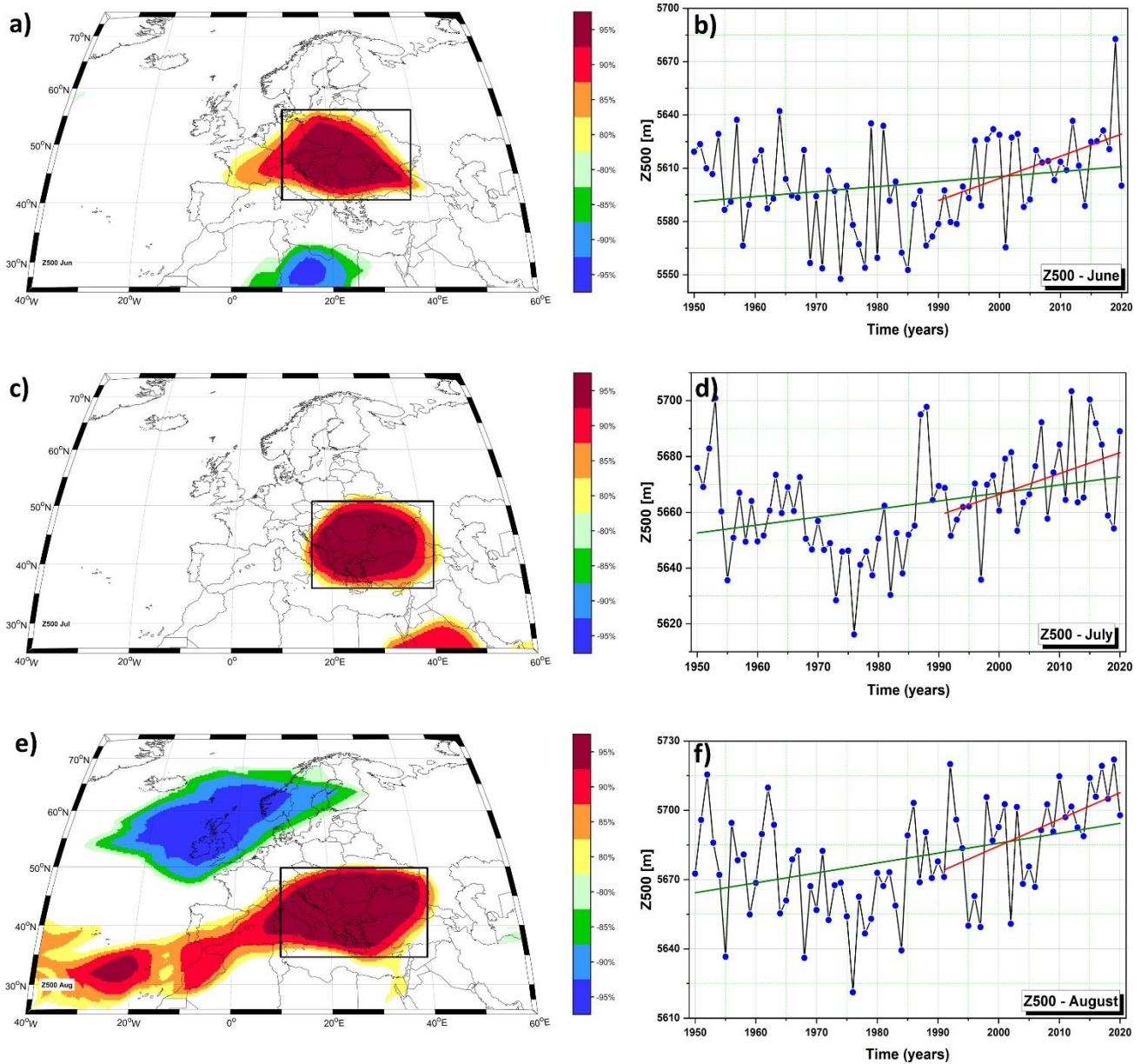
Figure 15. Stability maps of the correlation between monthly HWDI and monthly Z500 over the period 1950 – 2020 (left column) and the time series of monthly Z500 averaged over the black box in a), c) and e).

a) Stability map for June; b) The time series of June Z500 averaged overt the black box in a);

b) Stability map for July; d) the time series of July Z500 averaged overt the black box in c);

e) Stability map for August and f) the time series of August Z500 averaged overt the black box in e).

In a), c) and e) the regions where the correlation is positive for at least 80% of the 31-year windows are shaded with dark red (95 %), red (90 %), orange (85 %) and yellow (80 %). The corresponding regions where the correlation is significant, stable and negative, are shaded with dark blue (95 %), blue (90 %), green (85 %) and light green (80 %). The green (red) lines in b), d) and f) indicates the linear trend line of the monthly Z500 over the period 1950 – 2020 (1990 – 2020).

820